Review

Environmental Chemistry and Safety
DOI: 10.26599/ECS.2025.9600045
2025, 1, 96000045

Advances in research on ultra-low oxidant consumption: Fenton and Fenton-like systems

Kunyu Cai[1], Ghulam Hassan Abbasi[3], Hong Chen[1*], and Lindong Liu[1,2*]

[1]Interdisciplinary Research Centre for Agriculture Green Development in Yangtze River Basin, Department of Environmental Sciences and Engineering, International S & T Cooperation Base on Water Environmental Monitoring and Simulation in TGR Region, College of Resources and Environment, Southwest University, Chongqing 400716, China

[2]Yibin Academy of Southwest University, Sichuan 644005, China

[3]Institute of Agro-Industry & Environment, Faculty of Agriculture & Environment, The Islamia University of Bahawalpur, Bahawalpur, 63100,Pakistan

Abstract: Against the backdrop of green sustainable development, Fenton and Fenton-like reaction systems serve as crucial advanced water treatment technologies. A key research focus lies in exploring reaction pathways and mechanisms that minimize peroxide consumption while ensuring efficient degradation and detoxification of organic pollutants. In this review, we systematically outline strategies for achieving ultra-low peroxide consumption based on three key aspects of the reaction system: (i) Regulating non-radical oxidation processes mediated by $^1O_2$, high-valent metal species, and electron transfer process, leveraging their higher selectivity and longer lifetimes compared to radicals (e.g., $SO_4^{\bullet-}$ and $HO^{\bullet}$) to effectively reduce peroxide usage; (ii) Dynamically modulating reaction pathways and efficiently generating/utilizing non-radical reactive species through multiscale catalyst regulation and optimization; (iii) Guiding the precise design and economical selection of catalysts and AOPs based on organic pollutant substrate characteristics. Finally, this paper thoroughly examines key challenges and development directions for non-radical oxidation systems in practical applications. It aims to advance the engineering transformation of these technologies for real-world wastewater treatment, emphasizing their significant potential and application prospects as low-peroxide-consumption water treatment strategies. This review seeks to provide critical references and theoretical support for developing efficient and economical technologies for organic pollutant removal.

Key words: Ultra-low oxidant consumption; Non-radical pathways; Fenton and fenton-like systems; Advanced oxidation processes

Citation: Cai K Y, Abbasi G H, Chen H, et al. Advances in research on ultra-low oxidant consumption: Fenton and Fenton-like systems. *Environmental Chemistry and Safety*, 2025, 1, 96000045. https://doi.org/10.26599/ECS.2025.9600045

1. Introduction

With the acceleration of industrialization and urbanization, coupled with global population growth and rising living standards, vast quantities of complex and persistent organic pollutants (such as industrial wastewater, pesticides, and antibiotics) are being discharged into water bodies, posing a severe threat to global water resource security[1-3]. Although concentrations of these pollutants in natural water bodies are typically low, ranging from micromolar (μM) to nanomolar (nM) levels, their environmental persistence and bioaccumulation properties pose serious threats to ecosystems and human health[4]. Existing water treatment technologies, such as biological treatment and adsorption processes, demonstrate limited effectiveness against high-concentration, highly toxic pollutants, failing to meet practical application demands—particularly in terms of mineralization capacity[5]. Advanced oxidation processes (AOPs) have garnered significant attention in recent years for water treatment research and applications due to their high efficiency in removing refractory organic pollutants. Among these, the most widely applied Fenton and Fenton-like systems enable efficient degradation and detoxification of pollutants by activating various peroxides (e.g., H_2O_2, PMS, PDS, PAA) to generate diverse reactive species (RS)[6-8]. However, conventional oxidation processes generate highly reactive species based on free radicals, such as hydroxyl radicals ($HO^{\bullet}$) and sulfate radicals ($SO_4^{\bullet-}$), these radicals exhibit limited selectivity toward target pollutants in complex water bodies and readily produce toxic byproducts, potentially causing secondary pollution. More critically, these processes typically demand substantial chemical reagents and energy inputs. The intensive consumption of peroxides and low utilization efficiency constrain their widespread practical application, conflicting with sustainability and low-carbon goals[9-12]. Therefore, achieving efficient pollutant degradation while ensuring precise activation and efficient utilization of peroxides has become a key scientific challenge for advancing the practical application of AOPs.

Recent studies have reported oxidation processes generat-

Correspondence to: Chen H, chenhong@swu.edu.cn; Liu L D, lindongliu@swu.edu.cn

Received: September 16, 2025; Revised: October 10, 2025; Accepted: November 12, 2025

ing non-radical active species and their mechanisms, including singlet oxygen ($^1O_2$), highly oxidized metal species, as well as active complexes and catalyst-mediated electron transfer[13-15]. This non-radical oxidation within AOPs has garnered increasing attention in environmental science and chemistry literature, emerging as a significant research direction in advanced oxidation technology studies. According to literature statistics from 2015 to 2024, the number of related publications exhibits a pronounced exponential growth trend, with a fitted doubling time of approximately 2.34 years, indicating rapid development in this research area within environmental and chemical fields (Figure 1). Compared to traditional radical-based oxidation processes, non-radical oxidation exhibits distinct characteristics: (i) non-radical active species possess longer operational lifetimes; (ii) due to their moderate oxidative capacity, non-radical systems primarily induce selective reactions rather than complete mineralization; (iii) Their oxidation reactions exhibit higher selectivity, enabling more efficient recognition and degradation of target pollutants, along with enhanced resistance to interference in complex water bodies containing common inorganic ions and background organic matter[16-18]. These characteristics are particularly crucial for improving the utilization efficiency of various non-radical species triggered by peroxides, thereby reducing peroxide consumption (Figure 1). However, controversy persists regarding whether non-radical systems can effectively reduce peroxide consumption. This issue primarily stems from the slower reaction kinetics of traditional catalysts in non-radical pathways, often accompanied by higher energy consumption, which limits the efficient generation and utilization of non-radical active species[16, 19]. Furthermore, non-radical pathways exhibit stronger dependence on organic substrates. Gaining a deep understanding of the key factors influencing substrate selectivity holds significant guiding importance and practical value for identifying primary reaction pathways, elucidating oxidation mechanisms, and optimizing catalytic system design[20, 21].

This review focuses on non-radical systems activated by peroxides. First, in Section 2, we systematically summarize the currently reported non-radical activation mechanisms of peroxides, elucidating their advantages in achieving higher selectivity and longer-lived active species generation while reducing peroxide consumption. Subsequently, Section 3 comprehensively introduces approaches at micro-, meso-, and macro-scales for regulating multifunctional advanced oxidation systems. These methods effectively mediate non-radical pathways or achieve efficient generation and utilization of various non-radical active species triggered by peroxides, thereby enhancing peroxide utilization. Section 4 further explores the substrate-dependent characteristics of non-radical oxidation pathways in selective degradation processes, demonstrating the critical role of substrate influence. It emphasizes the necessity of designing and optimizing catalytic systems based on the substrate specificity of organic pollutants to enable targeted engineering. Finally, we outline key challenges and development directions for current non-radical oxidation systems in practical applications. This aims to advance their translation into real-world wastewater treatment while underscoring their significant potential as low-peroxide-consumption water treatment technologies.

2. Non-radical pathways with high peroxide utilization

Despite their high oxidation potentials (e.g., +2.08 V_{NHE} for PDS, +1.82 V_{NHE} for PMS, and +1.77 V_{NHE} for H_2O_2), peroxides exhibit very limited direct degradation efficiency for most organic pollutants due to kinetic limitations and molecular structural stability. This necessitates substantial peroxide dosing in practical applications, resulting in low utilization rates[19, 22]. Catalytically or energy-assisted activation of peroxides to generate reactive species (RS)—including both radical and non-radical RS—has been explored to enhance their reactivity and utilization. However, the short lifetime and poor selectivity of radical RS further constrain the efficient use of peroxides. In contrast, non-radical-based AOPs require significantly less peroxide due to their higher selectivity and longer lifetime. Thus, non-radical activation pathways offer a promising alternative for efficient peroxide utilization. Currently, three mainstream non-radical pathways have been extensively reported: electron transfer processes (ETP), singlet oxygen formation, and oxidation induced by high-valent metal species (HVMs).

2.1. Singlet oxygenation

Singlet oxygen ($^1O_2$) is widely recognized as one of the reactive oxygen species (ROS) with significant advantages in AOPs. Compared to hydroxyl radicals ($HO^•$) and sulfate radicals ($SO_4^{•-}$), $^1O_2$ exhibits stronger resistance to interference and a broader pH tolerance range in complex aquatic matrices, gar-

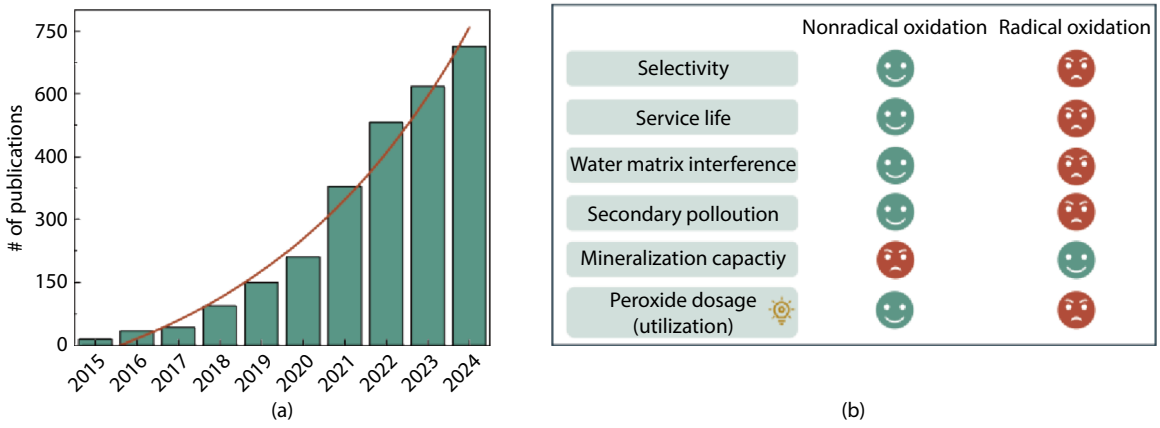

Fig. 1. (a) Publication trends on advanced oxidation processes based on non-radical pathways from 2015 to 2024; (b) Qualitative comparison of key features between nonradical and radical oxidation pathways.

nering extensive attention in recent years[23]. During reactions with pollutants, $^1O_2$ exhibits selective oxidation characteristics distinct from radicals. As a highly electrophilic and selective reactive oxygen species (ROS), $^1O_2$ primarily targets functional groups with high electron density or structural instability within pollutant molecules—such as aromatic rings, double bonds, and amino groups—through mechanisms like electrophilic addition or cycloaddition. This approach avoids nonselective attacks on coexisting substances or background components in water and reduces the formation of toxic intermediates (e.g., halogenated byproducts) from side reactions, thereby significantly decreasing the ineffective consumption of peroxides[16, 23-25]. Furthermore, $^1O_2$ exhibits a longer lifetime (approximately 2–4 μs in aqueous phase) and a greater diffusion radius (reaching tens to hundreds of nanometers), significantly outperforming HO• radicals (with lifetimes of only a few nanoseconds and diffusion radii under 10 nm). This enables $^1O_2$ to effectively participate in oxidation reactions within diffusion-limited regions of heterogeneous systems, demonstrating excellent adaptability and reaction persistence. Consequently, it enhances the probability of effective reactions with pollutant molecules[26, 27]. In summary, $^1O_2$ demonstrates greater stability and sustained degradation capability than free radicals in aquatic environments characterized by high salinity, strong buffering capacity, or complex organic pollutants. This makes it a key pathway for enhancing the selectivity of AOPs and improving the utilization efficiency of peroxides.

The generation of $^1O_2$ can be achieved through the spontaneous decomposition of peroxides or under catalytic activation conditions. However, its reaction kinetics are often constrained by factors such as temperature, pH, and catalyst surface activity, which influence its formation rate and yield. For instance, peroxymonosulfate (PMS) can generate $^1O_2$ via acid-base equilibrium (Equation 1) and subsequent reactions (Equation 2), but the overall rate remains low. While the self-decomposition of hydrogen peroxide (H_2O_2) (Equation 3) releases $^1O_2$, it typically requires external energy inputs such as elevated temperatures or UV irradiation, resulting in poor energy efficiency[28]. Therefore, introducing catalysts or energy assistance has become a key approach to enhance $^1O_2$ generation efficiency. Current studies indicate that the primary mechanisms for $^1O_2$ generation include: (i) Catalytically activated persulfates (PMS and PDS) generate $^1O_2$ via $SO_5^{\bullet-}$ or ($O_2^{\bullet-}$ intermediates (Equations 4–5)[29, 30]; (ii) $HO_2^{\bullet}$ generated from activated H_2O_2 reacting with ($O_2^{\bullet-}$ via proton-coupled disproportionation (Equation 5) or radical recombination (Equations 6–8). This mechanism is significantly accelerated in the presence of transition metal ions (e.g., Fe^{2+}) or carbon-based materials, but requires controlling H_2O_2 concentration to avoid quenching effects from its self-decomposition process[28, 31-33]. Furthermore, through catalyst optimization strategies (e.g., coordination adjustment, surface defect-guided activation, heteroatom doping), the efficient generation and release of $^1O_2$ can be further enhanced (achieving 100% selective production), improving the activation selectivity of peroxides. This enables pollutant oxidation at lower peroxide doses, which will be discussed in detail in the next section.

$$HSO_5^- + H_2O \leftrightharpoons SO_5^{2-} + H_3O^+ \quad (1)$$

$$HSO_5^- + SO_5^{2-} \rightarrow HSO_4^- + SO_4^{2-} + {}^1O_2 \quad (2)$$

$$2H_2O_2 \rightarrow 2H_2O + {}^1O_2 \quad (3)$$

$$4SO_5^{\bullet-} + 2H_2O \rightarrow 4HSO_4^- + 3{}^1O_2 \quad (4)$$

$$2O_2^{\bullet-} + 2H_2O \rightarrow {}^1O_2 + H_2O_2 + 2OH^- \quad (5)$$

$$O_2^{\bullet-} + \cdot OH \rightarrow {}^1O_2 + OH^- \quad (6)$$

$$O_2^{\bullet-} + HO_2^{\bullet} \rightarrow {}^1O_2 + HO_2^- \quad (7)$$

$$2HO_2^{\bullet} \rightarrow {}^1O_2 + H_2O_2 \quad (8)$$

Although the $^1O_2$ system demonstrates significant advantages in enhancing reaction selectivity and reducing peroxide consumption, it still faces numerous controversies and challenges in practical applications. First, the reaction rate constant of $^1O_2$ ($k \approx 10^2$–10^8 M^{-1} s^{-1}) is generally lower than that of radical species such as HO• and $SO_4^{\bullet-}$ ($k \approx 10^6$–10^{11} M^{-1} s^{-1}), limiting its degradation efficiency for less reactive pollutants like perfluorinated compounds and halogenated hydrocarbons[16]. Second, current $^1O_2$ detection methods predominantly rely on indirect approaches, such as electron paramagnetic resonance (EPR) or quencher (e.g., NaN_3, L-histidine), but their specificity and accuracy are susceptible to interference from other coexisting reaction intermediates. This may lead to overestimation of the $^1O_2$ contribution, obscuring the actual role of other reactive species in the system (such as $SO_4^{\bullet-}$ or high-valent metal oxygen intermediates), thereby introducing bias in the assessment of the 'low-consumption' effect[34, 35]. Furthermore, $^1O_2$ generation and stability are highly dependent on the catalyst's structural and environmental compatibility, while its dynamic regulation mechanisms and transfer pathways remain poorly understood.

2.2. High-valent metal induced oxidation

High-valent metal species (HVMs) represent a class of non-radical active species with potent oxidative capabilities, exhibiting strong electrophilicity and selectivity similar to singlet oxygen. Consequently, HVMs are frequently employed in fields such as biomimetic oxidation, biomedicine, and organic synthesis[36, 37]. Recently, research on HVMs (e.g., Fe(IV), Co(IV), Ni(IV), Cu(III), and Mn(V)) has significantly increased in environmental catalysis due to multiple advantages over radical oxidation pathways, including: (i) enhanced resistance to background aquatic matrix interference, maintaining stable activity in the presence of alcohols, natural organic matter (NOM), and common inorganic anions[38, 39]; (ii) extended lifetimes (e.g., Fe(IV) with lifetimes reaching 7–10 s)[40, 41]; (iii) Higher equivalent steady-state concentrations[42]; (iv) Enhanced substrate specificity and selectivity[43-45]. HVMs typically exist as metal-oxygen intermediates ($M^{(n+2)+}=O$) and degrade organic pollutants via hydrogen abstraction, oxygen transfer, and electron transfer pathways. Similarly, since the oxidative behavior of HVMs often targets specific electron-donating sites within pollutant molecules (e.g., amino groups, phenolic hydroxyls, sul-

fides, alkenes), they enable more precise targeted oxidation of electron-rich pollutants[46-48]. Furthermore, the straightforward generation pathway of HVMs—typically involving single-step redox reactions—often exhibits higher peroxide utilization efficiency than singlet oxygen. Specifically, direct redox reactions occur between peroxides and the metal active center, with nearly every peroxide molecule effectively contributing to HVMs formation. This process demonstrates a one-to-one redox reaction and enables controlled cyclic regeneration of the metal center. In contrast, $^1O_2$ generation often involves multi-step processes such as energy transfer and excited-state intermediates, leading to energy and reactant losses within the system. Therefore, in terms of generation pathway efficiency and oxidant conversion rate, the HVMs mechanism typically outperforms the $^1O_2$ pathway in peroxide utilization.

Unlike freely diffusing ROS, HVMs do not rely on free diffusion during reactions but instead achieve rapid electron coupling between surface metal active sites and pollutants at the interface. Consequently, HVMs exhibit distinct advantages in solid-liquid heterogeneous systems, making them suitable for spatially constrained environments such as channel catalysis and membrane interface reactions. They can maintain catalytic efficiency while significantly reducing the ineffective consumption of peroxides. However, the formation of HVMs is highly dependent on efficient electron transfer between metal ions or coordination centers and peroxides. Their activation pathways are influenced by multiple factors including metal valence states, ligand environments, and electronic orbital regulation[49], which ultimately determine whether HVMs can be effectively generated. Furthermore, the reaction kinetics of HVMs toward most organic pollutants typically exhibit low rates ($k \approx 10^2$–10^4 M^{-1} s^{-1}). Consequently, even under high utilization conditions, the overall removal efficiency of pollutants may remain limited[50-52]. Therefore, to fully leverage the advantages of HVMs in selectivity and lifetime, it is imperative to optimize catalyst design (e.g., coordination structure design and regulation of interfacial microenvironments) to achieve efficient generation and utilization of HVMs. This approach enables highly effective oxidative removal of target pollutants using lower peroxide doses[53-55].

2.3. Electron transfer process (ETP)

Recent studies indicate that the electron transfer process (ETP) demonstrates significant improvements in peroxide utilization efficiency compared to other oxidation pathways[56]. ETP enables either direct electron extraction from contaminant molecules (adjacent transfer) or indirect electron migration mediated by conductive catalysts (electron shuttle). In a typical ETP-driven system, the electron flow follows a well-defined pathway. When organic pollutants and peroxide molecules are co-adsorbed on the catalyst surface, the pollutant acts as an electron donor, transferring electrons either directly to the surface-activated catalyst–peroxide complex (proximal transfer) or indirectly through the conductive network of the catalyst (shuttle transfer). The catalyst thus serves as an intermediate electron bridge, facilitating bidirectional charge transport between the donor and acceptor. This electron-relay process enables efficient peroxide activation via the catalyst–peroxide complex, while simultaneously promoting pollutant oxidation at the solid–liquid interface. Notably, the ETP pathway differs from classical radical reactions in that the electron transfer is confined to interfacial charge-transfer steps rather than relying on the free diffusion or lifetime of transient reactive species, thereby exhibiting higher selectivity and lower peroxide consumption[57, 58]. Therefore, unlike active species generated through redox reactions between the catalyst and peroxides or other secondary reactions (e.g., radicals, $^1O_2$, and HVMs), ETP offers several technical advantages and unique characteristics. For instance: (i) Electron transfer in ETP systems does not occur spontaneously prior to pollutant introduction, meaning peroxides must accept electrons from pollutants to be effectively consumed, significantly enhancing peroxide utilization efficiency[59]; (ii) The formed surface oxidation complexes are essentially unaffected by half-life and independent of free diffusion processes, avoiding inefficient self-depletion[59, 60]; (iii) ETP systems exhibit high selectivity, determined by the electron-transfer potential of organic pollutants and the higher utilization efficiency of peroxides[61]; (iv) Similar to HVMs, the oxidation reactions triggered by ETP occur at the solid-liquid interface, i.e., interfacial catalysis. Under certain conditions, this constitutes the initial step in the polymerization degradation pathway of pollutants[62, 63]; (v) The stoichiometric ratio between consumed peroxides and target pollutants is low, significantly reducing chemical dosage requirements. For example, in peroxysulfate-based ETP mechanisms, the actual consumption ratio of peroxysulfate to organic pollutants approximates their theoretical stoichiometric ratio[61]. Consequently, these characteristics make ETP a more efficient pollutant degradation pathway with reduced peroxide consumption.

At least two critical considerations can be raised regarding these characteristics: the peroxide activation efficiency and pollutant oxidation efficiency within ETP are jointly influenced by thermodynamic properties (interaction strength) and kinetic factors (electron transfer and mass transfer efficiency). These are determined collectively by the physicochemical properties of both the catalyst and the pollutants. Optimization can be achieved by modifying catalyst properties and microenvironments, such as altering the catalyst's electronic characteristics to enhance electron transfer efficiency, increasing specific surface area, or designing spatial confinement (details in Sections 3 and 4). Typically, efficient mass transfer of reactants (peroxides and organics) in solution coupled with strong adsorption on the catalyst surface promotes ETP, leading to highly efficient peroxide activation and organic oxidation[64, 65]. Notably, ETP systems exhibit high peroxide utilization efficiency even at low peroxide doses. Conversely, excessive peroxide loading may cause superabundant adsorption, leading to surface adsorption competition or even active site shielding, thereby reducing catalyst conductivity and reactivity[66, 67].

Currently, the practical application of ETP remains in its early stages. Despite the advantages of ETP mechanisms, their apparent efficiency in reducing peroxide consumption may be influenced by matrix effects in real water systems. The presence of competing anions or natural organic matter can interfere with pollutant adsorption and electron transfer dynamics by occupying surface sites or scavenging reactive intermediates. Moreover, fluctuations in ionic strength and solution conductivity can alter the catalyst's electron mobility and surface potential, leading to decreased charge transfer rates. These fac-

tors often cause discrepancies between ideal laboratory observations and practical wastewater treatment outcomes. Integrating this mechanism into modular catalytic systems and developing engineering designs suitable for large-scale membrane or fixed-bed reactors will help accelerate its adoption. Furthermore, due to the relatively low redox potential of ETP systems (e.g., 0.6–1.2 V for peroxysulfate/carbon nanotube systems), their oxidation capacity for electron-withdrawing pollutants is limited, primarily relying on the oxidation of electron-donating pollutants[66]. Encouragingly, recent reports have demonstrated the sustainable degradation of organic pollutants with high ionization potentials (IP > 8.5 eV) via ETP mechanisms, attributed to rational catalyst design and optimization[68, 69]. These advances offer new insights for extending ETP mechanisms to broad-spectrum pollutant control while expanding the application scope for precise oxidation under low-peroxide-dose conditions.

2.4. Properties of peroxides

Common inorganic peroxides (PMS, PDS, and H_2O_2) can all initiate non-radical pathways. However, the molecular structure and bond energy characteristics of different peroxides largely determine their activation pathways and system applicability, significantly affecting their utilization efficiency in catalytic oxidation processes. Therefore, rationally selecting suitable peroxides is one of the key strategies for achieving efficient, low-dose non-radical systems. On one hand, PDS exhibits molecular symmetry and a relatively low peroxy bond dissociation energy (92 kJ·mol^{-1}), making it prone to homolytic cleavage under energy transfer processes (e.g., thermal or photoactivation) or transition metal activation conditions, preferentially generating highly reactive $SO_4^{\bullet-}$[19, 70]. However, under the influence of suitable catalyst electronic structures and interfacial environments, it still possesses non-radical transformation potential[71]. In contrast, the asymmetric structure confers stronger electrophilicity to PMS, enabling enhanced electron synergy and complexation with carbonaceous materials and metal catalysts. This facilitates the induction of high-valent metal formation or direct initiation of electron transfer processes[72, 73]. Additionally, PMS's smaller molecular size and lower steric hindrance improve its coverage on active sites within the catalyst surface, promoting selective oxidation at the solid-liquid interface. On the other hand, the structural symmetry and high peroxy bond dissociation energy (213.3 kJ·mol^{-1}) of H_2O_2 make its cleavage difficult under uncatalyzed conditions. It often relies on metal ions (such as Fe^{2+}) to activate and generate $HO^{\bullet}$, thereby favoring non-selective radical pathways[74, 75]. For the H_2O_2 system, a series of catalyst optimization strategies can also be employed to regulate non-radical pathways[76-78]. Overall, PMS exhibits superior interfacial reactivity and selective oxidation potential in non-radical oxidation systems, while the non-radical activity of PDS and H_2O_2 relies more heavily on catalyst design and interfacial environment control. This underscores the critical role of matching peroxide type with the catalytic system for enhancing peroxide utilization efficiency.

3. Catalyst modulation strategies with high peroxide utilization

How to reduce the consumption of peroxides while ensuring efficient reactions has become a critical issue in current environmental remediation and green development. Catalysts play a central role in this process, primarily by enhancing the activation efficiency of peroxides and regulating reaction pathways. On one hand, catalysts lower the reaction energy barrier between peroxides and reactants, overcoming the energy obstacles encountered during peroxide activation and thereby accelerating the formation of reactive species[79, 80]. On the other hand, catalysts can also regulate the types of active species generated after peroxide activation and their reaction pathways. For instance, certain catalysts selectively activate peroxides to generate non-radical species (e.g., $^1O_2$, highly oxidized metals, surface complexes), circumventing the low selectivity and byproduct issues prevalent in radical pathways, thereby improving peroxide utilization. However, the activity of catalysts mediating non-radical pathways remains relatively limited. Enhancing their catalytic performance or altering reaction mechanisms is necessary to achieve efficient generation and utilization of non-radical species[81-83]. Notably, catalytic performance and mechanisms depend not only on the intrinsic properties of active sites but also on the synergistic regulation of multiscale environmental factors such as mass transfer behavior, stability, and local reaction kinetics[84-86]. Consequently, a series of engineering strategies have been employed to optimize the overall performance of various heterogeneous catalysts. These include: (i) modulation at the atomic/molecular level (e.g., varying coordination environments, doping-induced electronic states); (ii) adjustment of interfacial and complex surface physicochemical properties (e.g., localized pH, restricted reaction environments due to nanoconfinement mechanisms); (iii) design and application of integrated systems incorporating filters, membranes, or catalytic beds [87-90]. These strategies, operating at different levels, regulate multifunctional advanced oxidation systems to effectively mediate non-radical pathways or achieve efficient generation and utilization of various non-radical species triggered by peroxides. Compared to traditional Fenton and Fenton-like systems, the utilization of peroxides is significantly enhanced.

3.1. Atomic/molecular-level regulation

Atomic/molecular-level regulation of catalysts represents an effective strategy for improving peroxide activation efficiency and tuning reaction pathways, thereby contributing to reduced peroxide consumption in Fenton-type systems.[91-93]. Such approaches not only focus on modulating electronic structures and energy level distributions through precise coordination structure control of active sites but also incorporate heteroelement doping to enhance reactivity, providing effective pathways for improving intrinsic catalyst activity and reaction kinetics. For instance, in in situ generated active species (such as surface active complexes and highly oxidized metal species), catalysts typically function as electron transfer mediators or interfacial activators. Their conductivity, electron distribution (e.g., d-band center position), and coordination state directly determine electron transfer efficiency and utilization, thereby influencing peroxide utilization[94-96]. Furthermore, the aforementioned multiscale regulation methods can also selectively enhance the generation efficiency of non-radical species like singlet oxygen, compensating for their relatively

low reaction kinetics compared to radicals ($k \approx 10^6$–10^{11} M^{-1} s^{-1}). For instance, the kinetic rates for $^1O_2$ ($k \approx 10^2$–10^8 M^{-1} s^{-1}) and $M^{(n+2)+}=O$ ($k \approx 10^2$–10^4 M^{-1} s^{-1}) exhibit deficiencies[97-99]. In this subsection, we systematically explore optimization strategies for catalysts commonly used in Fenton-type systems at the microscopic level, aiming to elucidate the key mechanisms underpinning the utilization of low-consumption peroxides.

3.1.1. Modulation of coordination structure

Benefiting from maximum atomic utilization, uniform active sites, and tunable electronic structures, carbon-based single-atom catalysts (SACs) demonstrate significant application potential for achieving efficient pollutant removal and reducing peroxide dosage[80, 100-102]. Specifically, the geometry and electronic structure of the metal active center, along with the reaction adsorption energy, are tunable and influenced by the local microenvironment formed between the metal site and the carbon support. This enables SACs to dynamically regulate reaction pathways and promote low-dose, highly selective non-radical reaction processes. Key parameters governing this local microenvironment regulation include the characteristics of the metal center, the number and type of coordinating atoms, and the metal-support interactions[80]. For instance, different metals (such as transition metals Fe, Co, Cu, and Mn) exhibit distinct reactivity and selectivity in peroxide activation and active species generation[103, 104]. Gao et al. demonstrated that the activation trend for PMS with selective $^1O_2$ generation follows: Fe-SAC (88%) > Co-SAC (79%) > Mn-SAC (70%) > Ni-SAC (62%) > Cu-SAC (56%). Among these, Fe-SAC exhibits moderate and near-average Gibbs free energy at each reaction step in the $^1O_2$ generation pathway, thereby promoting efficient $^1O_2$ production and high utilization[105]. Furthermore, Miao et al. synthesized a series of 3d transition metals anchored on CNTs (M-N-CNTs) catalysts. Among these distinct single-atom M-N sites, the high effective magnetic moment of the high-spin state (Co-N) was found to favor d-orbital overlap with PMS at the metallic active site, effectively forming Co-PMS* complexes. This efficiently triggers the electron transfer pathway (ETP) rather than the conventional radical decomposition pathway. This system features an oxidation complex with a high oxidation potential and enhanced electron transfer capability. Upon addition of an appropriate amount of organic pollutants, it immediately promotes the utilization efficiency of peroxydisulfate, thereby significantly reducing peroxydisulfate input[106].

The next key focus in regulating the atomic/molecular-level microenvironment of the catalyst center's first layer is altering coordination number. The metal-nitrogen tetracoordinate structure (denoted as M–N_4), frequently reported in previous studies, does not always achieve optimal adsorption energy during PMS activation, preventing maximized PMS utilization. Recently, methods to adjust the coordination number of nitrogen atoms have emerged as an effective strategy. For instance, constructing unsaturated coordination by reducing the nitrogen coordination number in cobalt single-atom catalysts (Co-N_2) enables a shift in the PMS activation pathway. In this case, The effective yield of $^1O_2$ in this system is nearly three times higher than that in the Co-N_3 system, replacing the original radical species as the primary contributor. This is because the reduced coordination number alters the electron density near the Fermi level of the Co atom, leading to enhanced PMS adsorption and increased specific activity. This further boosts the yield of non-radical species ($^1O_2$), which becomes the main contributor to organic matter degradation, thereby reducing PMS consumption.(Figure 2)[107, 108]. Conversely, introducing non-planar coordination to increase coordination number disrupts electronic distribution symmetry, creating a more three-dimensional coordination environment. This promotes the selective generation of non-radical RS species (e.g., $Fe^{IV}=O$, $^1O_2$, and PMS complexes)[109-111]. A consistent outcome is that PMS utilization efficiency is significantly enhanced compared to conventional SACs (achieving over 90% utilization), with reduced undesirable consumption. This improves the catalyst's overall reaction performance and operational stability in complex aqueous environments.

3.1.2. Doping modification

Doping, as a key strategy for regulating catalyst composition and structure at the atomic/molecular scale, has been widely applied to confer new functions or optimize the performance of catalysts[112-114]. Since dopant atoms typically possess distinct properties from intrinsic atoms (e.g., electronegativity), introducing heteroatoms via direct chemical bonds or long-range interactions readily modulates the physicochemical properties (e.g., electron density) of catalytic active sites. These alterations may influence binding strengths and adsorption energies with reactants (peroxides and organics) and intermediates, thereby affecting catalytic behavior. This represents an effective strategy for dynamically regulating reaction pathways and enhancing peroxide utilization (Figure 3)[115-117]. For instance, boron atoms with lower electronegativity exhibit

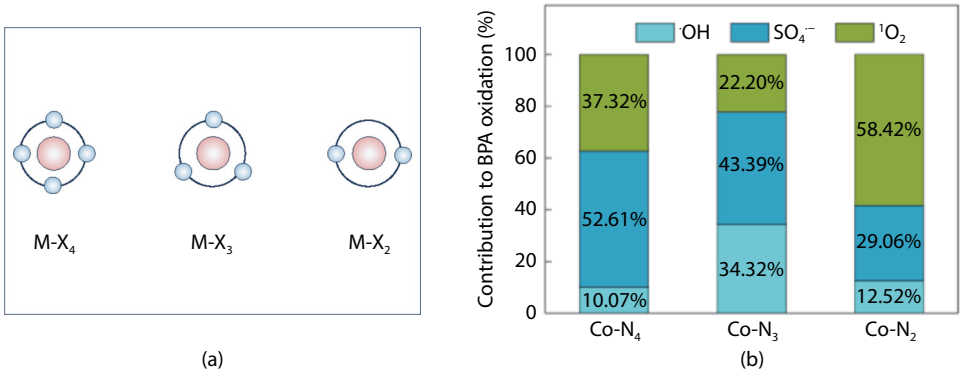

Fig. 2. (a) The metal center possesses atoms with different coordination numbers; (b) Contribution of various ROS to BPA oxidation in Co–N_x/PMS systems. Reproduced with permission.[107] Copyright 2022, Wiley-VCH Verlag.

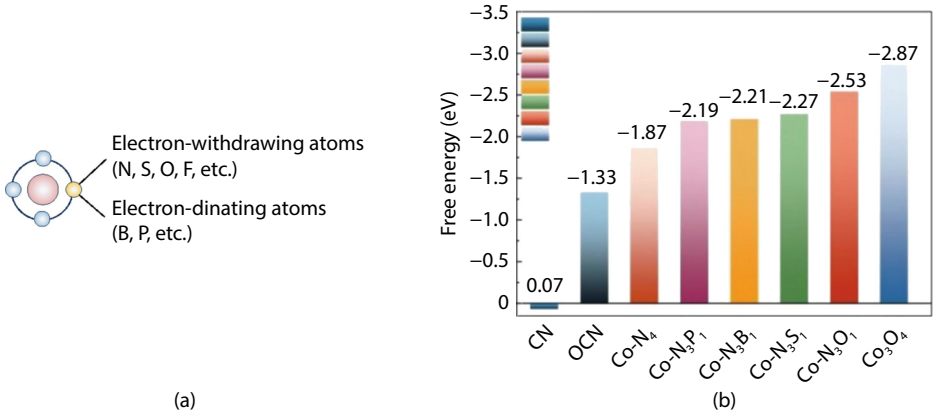

Fig. 3. (a) Different non-metal coordination induced by doping; (b) The adsorption energy of Co at the molecular level under different doping configurations. Reproduced with permission.[136] Copyright 2022, John Wiley and Sons Ltd.

electron-withdrawing capabilities. Following long-range interactions with Cu active sites, they reduce the electron density at Cu sites and lower the d-band center, thereby optimizing the adsorption energy for PMS activation. This facilitates efficient electron transfer from Cu-SAC to PMS, generating high-valent copper-oxygen species[91]. Modulating the coordination of boron atom doping in the first layer can also induce asymmetric electron distribution, thereby generating a strong local electric field. Under this field, coupled electron-proton transfer processes are enhanced, further enabling O–O and O–H bond cleavage and efficient electron transfer to selectively generate Co^{IV} = O. Compared to radical systems like CoN_4, the CoB_1N_3 framework efficiently oxidizes electron-rich pollutants while exhibiting strong resistance to inorganic interfering ions and humic acids in substrates, achieving higher PMS utilization[99]. Additionally, other dopant atoms such as fluorine, oxygen, nitrogen, and sulfur—which possess higher electronegativity—can fine-tune catalytic activity while stabilizing positively charged intermediates during catalysis, thereby promoting low-energy, non-radical-dominated oxidation pathways[118, 119].

Furthermore, different adsorption configurations (such as distinct adsorption sites) may lead to variations in activation pathway selectivity[120], offering new opportunities for dynamically regulating the transition from radical pathways to nearly 100% non-radical pathways. Taking the adsorption configuration of PMS as an example, when it selectively adsorbs terminal oxygen at electron-depleted active sites, it favors the formation of the $SO_5^{\bullet-}$ intermediate, thereby selectively generating $^1O_2$. Experiments confirm that this specific unit adsorption pattern enables nearly 100% selective $^1O_2$ generation[98, 121]. This is attributed to the introduction of non-metallic atoms with differing electronegativity, which alters the electron density distribution at the metal active site, thereby modulating the adsorption configuration of PMS[122]. However, single-site catalysts face inherent limitations in complex reaction systems: (i) their adsorption behavior is constrained by linear scaling of adsorption energy due to structural uniformity, and competition among multiple reaction intermediates at the same site hinders achieving ideal thermodynamic equilibrium between adsorption, activation, and desorption; (ii) Limited active site density restricts reactant diffusion and electron transfer efficiency[87, 123]. To overcome these bottlenecks, doping strategies based on dual-active-site synergistic mechanisms have emerged as a key research direction for enhancing peroxide activation efficiency[124, 125]. This approach combines the advantages of single-active-site catalysts while enabling synergistic interactions between two active sites. For instance, to circumvent the single-adsorption mode that triggers O–O cleavage and inevitably generates various radicals[126, 127], Wang et al. optimized the adsorption and peroxide activation pathways by introducing a Fe–Co dual site formed by a neighboring Co site around a single-atom iron active center, enabling simultaneous adsorption of both terminal oxygen atoms of PMS[128]. Under bisite synergy, electron rearrangement within the adsorbed PMS* complex is enhanced by slight O–O bond elongation. This optimization drives exclusive selectivity toward the ETP pathway (approaching 100% ETP), thereby significantly improving PMS utilization.

The formation of dual reaction centers with electron-rich/electron-deficient microdomains through doping-induced electron nonuniform distribution or the construction of electron transfer bridges can effectively guide surface electron migration, representing another effective strategy for reducing peroxide consumption[129, 130]. Fundamentally, such dual reaction center (DRC) catalysts operate through a similar mechanism: electron-rich sites accept electrons from pollutants and transfer them to electron-deficient sites, which then utilize these electrons to activate peroxides. Through this mechanism, peroxides are no longer ineffectively decomposed but instead act as oxidants that combine with electrons to generate various reactive oxygen species for further oxidation of organic pollutants. This mechanism, where pollutants serve as electron donors to replace excess peroxide consumption, significantly reduces peroxide dosage (i.e., H_2O_2 consumption is 6-8% of that in conventional Fenton-like systems)[131]. Beyond externally added peroxides, recent studies indicate that certain DRC catalysts, when induced by trace amounts of PMS or H_2O_2, can harness pollutant electrons and natural dissolved oxygen (DO) to achieve H_2O_2 amplification (i.e., in situ H_2O_2 generation) and efficiently remove pollutants. The generated H_2O_2 further participates in redox processes to enhance pollutant removal efficiency[132-134]. Consequently, this mechanism offers a novel perspective for addressing high energy consumption in water purification and substantially reducing peroxide consumption. Lu et al. designed a CZO catalytic system by doping Cu into the ZnO lattice. Driven by non-consumable H_2O_2, this system opens mass transfer pathways on the Cu-ZnO sur-

face and lowers the activation energy barrier for endogenous substances. Consequently, electrons and energy from pollutants are efficiently utilized to activate DO, enabling highly efficient catalytic degradation reactions at H_2O_2 concentrations ranging from 0 to 2.6%[135].

In summary, the key mechanisms involved in doping strategies within Fenton-like systems primarily include: (i) electronic effects, (ii) adsorption effects, and (iii) synergistic effects. Fundamentally, these effects are interconnected and mutually reinforcing, forming a multidimensional regulatory system that collectively drives the dynamic adjustment of reaction pathways and the efficient generation and utilization of non-radical RS.

3.2. Interface/surface modulation

The next research focus lies in optimization strategies for catalysts at the mesoscale level. At this scale, key regulatory approaches include nanoconfinement effects, localized pH modulation, and design of catalyst morphology and size. These methods emphasize surface and interfacial regulation of catalysts, influencing reaction pathways and catalytic performance. The three strategies demonstrate synergistic potential in spatial confinement, interfacial microenvironment control, and geometric configuration adjustment. This offers novel approaches to overcoming current kinetic and thermodynamic bottlenecks limiting the efficient utilization of peroxides, thereby advancing the practical application of various Fenton-like systems in wastewater purification.

3.2.1. Confinement effect

Fundamentally, the catalytic performance of heterogeneous catalysts is directly influenced by intermolecular interactions, spatial configuration, and intrinsic electronic arrangement. These critical factors can be effectively modulated through nanoconfinement effects, thereby driving kinetically unfavorable reactions—which are difficult to proceed under conventional conditions—toward the target direction with enhanced efficiency [137, 138]. The nanoconfinement effect regulates the microenvironment around active sites through spatial restriction, exhibiting unique advantages over unconstrained catalysts, including but not limited to the following aspects: (i) enhancing active site exposure and demonstrating significant selective accessibility, i.e., increasing the probability of effective contact with target reactants while achieving size exclusion of non-target molecules; (ii) promoting reactant enrichment in localized regions and improving mass transfer efficiency; (iii) Electron rearrangement and structural regulation induced by spatial confinement effectively lower the activation energy barrier and optimize interfacial electron coupling between the catalyst surface and adsorbed reaction intermediates[139-142]. Specifically, the effective active radius of ROS is extremely limited (<200 nm) (Figure 4), resulting in low utilization efficiency of peroxides. Nanoconfinement effects can encapsulate reactants (peroxides and organic compounds) within critical diffusion lengths (<200 nm), thereby strengthening interactions between peroxides and active sites and enhancing collision efficiency between active species generated at the catalytic interface and target pollutants. These effects collectively promote accelerated reaction kinetics and higher peroxide utilization (Figure 4)[143-145]. Liu et al. constructed a microenvironment with reactant enrichment and electronic regulation capabilities by confining Co_3O_4 nanoparticles within carbon nanotube channels[146]. Density functional theory (DFT) calculations confirmed that synergistic metal-support interactions and reactant enrichment effects facilitate efficient internal electron transfer between the catalyst and PAA, promoting directed $^1O_2$ generation. Subsequently, enriched pollutant molecules are rapidly targeted by fresh $^1O_2$ generated at active sites, enhancing $^1O_2$ utilization. Furthermore, for the oxidation pathways occurring at the interface (HVMs and ETP), mass transfer of peroxides and organic matter from the liquid phase to the catalyst surface is the rate-limiting step. Within nanoconstrained structures, reactants are confined to nanoscale spaces, altering their interaction kinetics, diffusion rates, and reactivity. This confinement drives their motion, accelerating mass transfer and enabling lower peroxide consumption[147, 148]. Interestingly, confinement effects can also induce pathway shifts toward non-radical pathways. Spatial confinement modulates charge distribution and triggers enhanced binding forces between reactants and catalysts, narrowing the energy gap required for electron transfer—key drivers of ETP oxidation. Achieving 100% ETP selectivity significantly enhances peroxide utilization, reduces operational costs, and effectively minimizes potential ecological impacts[149]. For instance, Meng et al. effectively optimized the surface electronic structure by confining cobalt active sites within mesoporous silica nanopores. This confinement system exhibits enhanced PMS deprotonation binding capacity and elevated energy barriers, suppressing radical generation from PMS cleavage. This prioritizes the conversion of PMS into surface-activated PMS* complexes, thereby shifting the reaction mechanism from a radical pathway to a non-radical mechanism dominated by ETP. Combined with the reactant enrichment effect and accelerated interfacial mass transfer, this system significantly increased PMS utilization from 61.8% in the non-confined system to 96.6%[148].

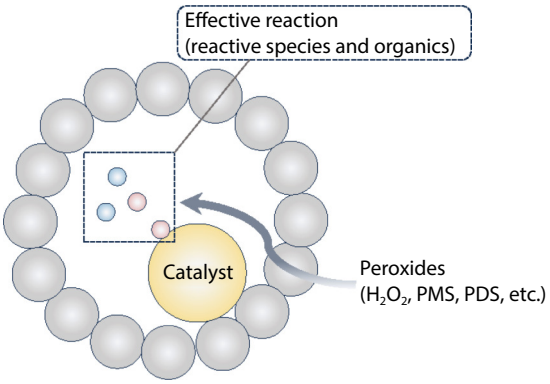

Fig. 4. The confinement effect enables the enrichment of reactants, thereby promoting the generation of reactive species and their efficient reactions with organic compounds.

3.2.2. Local pH modulation

Generally, catalytic systems based on metal-derived catalysts are highly susceptible to pH changes in aqueous solutions, leading to a significant decline in catalytic performance. For example, heterogeneous Fenton systems based on transition metals or metal oxides face issues such as active site loss (e.g., Fe^{2+} hydrolysis), self-decomposition of H_2O_2, and catalytic cycle inhibition at near-neutral or higher pH values, resulting in low H_2O_2 utilization[150-152]. Local pH refers to the acidity or alkalinity within specific microenvironments within a reaction sys-

tem (e.g., catalyst surfaces, nanopores), where distinct physicochemical properties and phase behaviors emerge compared to the bulk solution. Recent studies indicate that precisely designing catalyst surface charge characteristics or controlled-release components can form dynamic microzones with optimal pH at reaction interfaces. This approach overcomes pH limitations in pollutant remediation and enhances peroxide utilization (approaching 100%)[92]. For instance, certain carbon-based materials or metal-organic frameworks possess high specific surface areas, excellent stability, and abundant oxygen-containing functional groups[153, 154], making them ideal platforms for synthesizing functional hybrids or composites with tunable properties. Xu et al. synthesized a catalyst with localized pH-modulating capability by bonding graphene oxide (GO) onto a metal oxide (Figure 5)[155]. Hydroxyl and carboxyl groups on the GO surface act as proton sources, dynamically dissociating protons in response to the acidity of the bulk solution. This creates an acidic microenvironment (pH = 3-5) at the reaction interface, enabling the system to maintain high contaminant removal efficiency across a broad pH range of 3.0–10.0. Furthermore, electron transfer from the metal oxide to H_2O_2 is modulated by these oxygen-containing functional groups[156], enhancing the metal site's electron-donating capacity and strengthening its binding affinity with H_2O_2. This promotes electron transfer processes (ETP) mediated by surface-bound H_2O_2* complexes, achieving high H_2O_2 utilization[155]. Furthermore, layered double hydroxides (LDHs) are frequently employed to modulate local pH microenvironments. Hydroxides stabilize pH through self-dissociation or rapid reactions with H^+/OH^- in solution, thereby promoting the stable formation of non-radical species and the effective oxidation of organic pollutants, ensuring high peroxide utilization. For instance, in the CoMg-LDH/PMS system, rapid proton transfer and ionized OH^- around catalytic sites create an alkaline microenvironment (pH = 8-10). This promotes PMS protonation while suppressing deactivation of active Co species in protonic conditions, thereby accelerating $Co^{IV}=O$ formation. Compared to the unmodified system ($Co(OH)_2$/PMS), both PMS utilization (approximately 70%) and pollutant mineralization rate (41.7%) were significantly enhanced[157].

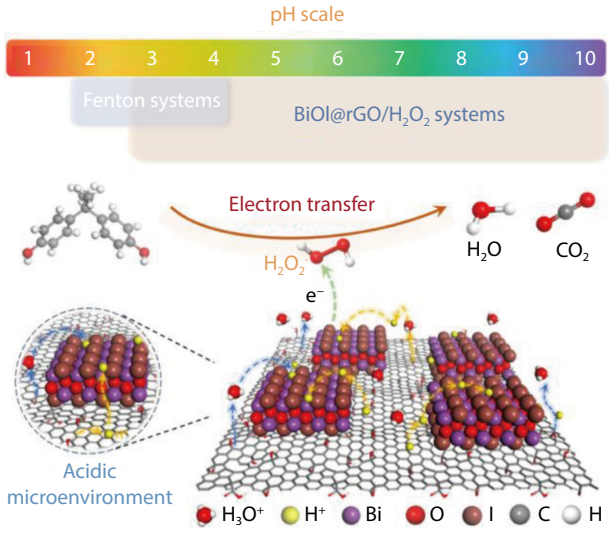

Fig. 5. By bonding graphene oxide, a local acidic microenvironment is created, thereby enabling the heterogeneous Fenton (BiOI@rGO/H_2O_2) system to sustainably degrade organic pollutants over a wide pH range (3.0–10.0). Reproduced with permission.[155] Copyright 2025, PERGAMON-ELSEVIER SCIENCE LTD.

In terms of application scope, constructing acidic microenvironments on iron-based heterogeneous catalysts overcomes bottlenecks such as dependence on acidic conditions and iron sludge formation, thereby significantly expanding the applicability of Fenton technology in practical wastewater treatment[158-160]. Reports have shown that MoS_2 can act as an effective co-catalyst to enhance Fenton-type reactions. Its unsaturated sulfur atoms exhibit proton-accepting properties, enabling the adsorption of H^+ ions from the solution and the formation of a relatively stable acidic microenvironment on the catalyst surface, which may contribute to an extended operational pH range[152, 161-163]. The multifunctional valence transition between Mo^{6+}/Mo^{4+} species further accelerates the rate-limiting step (i.e., Fe^{3+}/Fe^{2+} cycle), ensuring stable iron ion cycling on the slipping plane. This catalytic system not only enhances H_2O_2 utilization but also significantly reduces iron sludge formation, consuming H_2O_2 at levels 1–2 orders of magnitude lower than conventional Fenton systems[164-166]. Consequently, Fenton systems regulated by acidic microenvironments exhibit economical peroxide consumption and high stability, which is particularly crucial for expanding the applicability of Fenton technology in real-world wastewater treatment.

3.2.3. Morphology and size modulation

Designing nanocatalysts with specific dimensions and morphologies is an effective strategy for inducing more active sites and enhancing non-radical-based catalytic reactions, resulting in economical peroxide consumption. For instance, designing catalytic materials with distinct structural dimensions — such as nanotubes, nanosheets, and nanospheres —can enhance catalytic performance beyond conventional approaches, thereby improving peroxide utilization. This is attributable to the unique properties of these dimensional structures: (i) highly exposed active sites, (ii) enhanced mass transfer efficiency, and (iii) optimized electron transport pathways. Recently, an increasing number of two-dimensional (2D) sheet-like nanomaterials have been successfully synthesized from their bulk crystalline counterparts. Compared to their bulk counterparts, 2D nanosheets provide a larger reaction interface and more active sites for reactant contact, amplifying the complexity of adsorption and electronic interactions involved in the subtle interactions between reactants and catalysts[167-169]. Consequently, these two-dimensional nanoplate structures can effectively activate peroxides, enabling the rapidly generated non-radical RS to oxidize target pollutants, achieving high peroxide utilization rates (above 75%)[170]. However, bulk metallic materials (e.g., metal oxides) exhibit poor bulk conductivity and face challenges such as severe agglomeration of metal particles and insufficient morphology control during preparation, resulting in slower reaction processes. Most require carrier materials to design specialized structures[171, 172]. In contrast, carbon-based materials possess high electrical conductivity, diverse hybridized carbon (sp^2/sp^3), functional groups, and defects. They are commonly used to prepare catalytic materials with diverse dimensional structures (0D-3D) or as carrier materials for catalysts. For instance, the π electrons in sp^2-hybridized carbon on graphene nanosheets enhance the adsorption of perox-

ides and organic compounds, thereby promoting non-radical oxidation processes without generating radicals[173]. Carbon nanosheets with a high sp^2/sp^3 carbon hybridization ratio exhibit outstanding ETP activity, significantly enhancing peroxide utilization[174]. Furthermore, three-dimensional (3D) nanoporous carbon materials feature highly interconnected nanoscale pore networks extending throughout the 3D structure, exhibiting larger specific surface areas (can exceed 3000 $m^2\ g^{-1}$), tunable porous architectures, and surface chemistry. The uniform pore network and mesopore size exclusion (approximately 11 nm) prevent agglomeration and ensure efficient mass transport of target pollutants, enabling rapid adsorption to trigger the ETP process. Complete removal of various recalcitrant micropollutants can be achieved even at low PMS doses when treating complex aqueous matrices[175, 176]. Notably, combining these superior morphologies with strategies such as heteroatom doping, functional group modification, and defect engineering further modulates the catalyst's electronic structure, surface charge distribution, and adsorption energy, enhancing its reaction selectivity and efficiency in non-radical oxidation pathways.

3.3. Peroxide-efficient amplification module

Beyond rational catalyst design and microenvironment regulation, reactor design and effective immobilization strategies also play a crucial role in optimizing peroxide activation efficiency. Notably, the development of these reaction systems enables optimization of mass transfer kinetics and stabilization of active sites, which is essential for maintaining highly efficient and stable catalytic performance under operational conditions[177-179]. Various catalytic modules have been reported, such as catalytic membranes/filters, catalytic beds, and catalytic columns[180]. These laboratory-scale examples have significantly advanced the scaled-up implementation of Fenton and Fenton-like processes using diverse nanocatalysts, providing critical proof-of-concept for applying cost-effective peroxide-consuming systems to practical environmental remediation applications (e.g., pilot-scale and engineered-scale deployments).

3.3.1. Catalytic membrane/filter

Traditional suspended powder catalysts exhibit significant drawbacks in practical water treatment applications, including recovery challenges stemming from difficult solid-liquid separation, active site masking due to particle agglomeration, and limited mass transfer efficiency. Although laboratory-scale batch-sequential reactors can partially mitigate these issues, they commonly suffer from low treatment efficiency and additional consumption of peroxides. In contrast, catalytic modules integrating these nanoparticles, ultrafine nanoclusters, or single-atom catalysts onto membranes enable stable catalyst loading while maintaining high reactivity[181-183]. Notably, two-dimensional (2D) materials possess atomically thin monolayer structures. Layered membranes constructed from 2D materials — such as graphene and its derivatives, titanium dioxide nanosheets, and molybdenum disulfide nanosheets —exhibit multi-layered stacking structures with controllable interlayer spacing between adjacent nanosheets[184-186]. This unique spatial configuration induces directed, rapid transport of micropollutants and peroxides within membrane nanochannels, generating localized concentration polarization effects. This significantly shortens the diffusion distance of reactants to the catalyst surface and enhances the exposure and utilization of active species(Figure 6)[187-189]. However, in practical operation of catalytic membranes, membrane fouling remains a core challenge limiting flux stability and service life[190]. One limitation arises from natural organic matter (NOM) in real water samples, which consumes non-selective ROS in large quantities, reducing the available concentration of active species and thereby increasing the demand for peroxides. Simultaneously, the accumulation of NOM and degradation byproducts on the membrane surface forms a fouling layer that significantly accelerates the membrane fouling process [191, 192]. Recent studies demonstrate that, unlike conventional membrane structures, catalytic membranes with nano-confinement effects exhibit superior anti-fouling resilience against NOM permeation by precisely controlling pore size distribution. This characteristic not only effectively prevents the deactivation of catalyst active sites through coverage but also suppresses the non-target quenching of reactive species such as free radicals[193-195]. This unique reaction confinement enhances the selectivity of radical-driven AOPs, thereby significantly improving peroxide utilization. Tian and colleagues enhanced water flux by increasing the interlayer free spacing, maintaining excellent membrane permeability (>100 LMH/bar) while achieving efficient organic pollutant degradation and high mineralization rates (70.9%). This partially overcomes the trade-off between membrane permeability and selectivity[196]. Consequently, compared to conventional heterogeneous Fenton-like systems, these catalytic membrane structures —combining confined catalytic effects with hydrodynamic regulation —enable economical catalyst dosages (less than one-twentieth) and peroxide doses (<15%) while maintaining high pollutant removal efficiencies[182].

3.3.2. Catalytic bed/tower

Catalytic beds/towers are packed with inert solids or granular

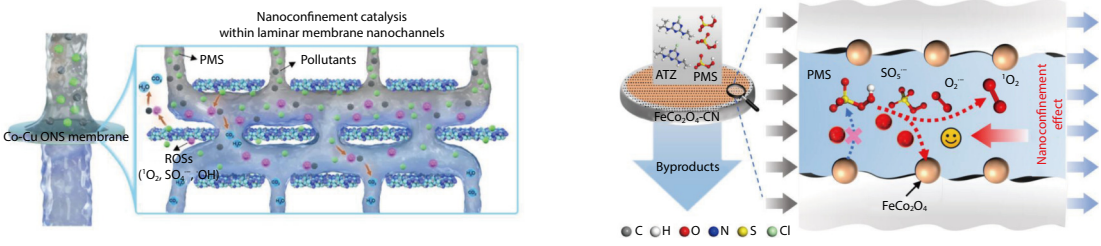

(a) (b)

Fig. 6. (a) Schematic illustration of the pollutant degradation mechanism in the Co–Cu ONS membrane/PMS system with a nano-confinement effect. Reproduced with permission.[186] Copyright 2022, Elsevier; (b) A flow-through structured ceramic membrane embedded with nanoconfined $FeCo_2O_4$ ($FeCo_2O_4$–CM) for PMS activation. Reproduced with permission.[187] Copyright 2024, American Chemical Society.

active catalysts, employing either fixed packing or fluidized (e.g., fluidized bed) gas/liquid-solid multiphase mixing modes[181, 197-199]. Compared to conventional reaction systems, catalytic bed/tower systems significantly enhance pollutant degradation kinetics and reduce peroxide consumption by intensifying mass transfer efficiency and optimizing reaction interface conditions. Recent pilot-scale studies have demonstrated that heterogeneous PMS-based catalytic systems, such as CuFeMnO/PMS reactors, can achieve stable COD and phenol removal (50–70% efficiency over 188 h) from real secondary effluents, with low catalyst leaching and moderate treatment cost (≈126.8 RMB/m^3), confirming their practical stability and economic feasibility for complex wastewater treatment (Figure 7)[200]. In addition, Zhang et al. achieved comparable organic pollutant degradation efficiency in a packed-bed reactor using their granular N-C/Co@PSS catalyst, while consuming only one-third the peroxymonosulfate (PMS) dosage compared to batch experiments[201]. However, macroparticles formed from powder catalysts are prone to mechanical breakage or structural collapse during prolonged operation, leading to abnormal reactor pressure drop and catalytic activity decline. In contrast, physically or chemically loading the active component onto supports such as porous ceramic beads, glass beads, or activated carbon not only enhances the catalyst's mechanical stability but also improves peroxide utilization efficiency by optimizing active site distribution and mass transfer pathways[200, 202-204]. Li and colleagues employed three-dimensional polyvinylidene fluoride (PVDF) foam as a support, constructing cobalt-based catalytic modules via in-situ growth technology and integrating them into a dynamic packed-bed reactor system. The composite carrier's unique mesoporous structure and superhydrophilic properties not only significantly increased active site accessibility but also maximized PMS activation efficiency by reducing mass transfer resistance. This system demonstrated outstanding treatment performance and operational stability when addressing challenging environments such as high-salinity wastewater, turbulent conditions, and complex matrix wastewater[205].

It should be noted that when scaling up laboratory-scale catalyst integrated systems for pilot-scale or industrial processing, a comprehensive assessment of actual environmental factors and operational costs is crucial for achieving the economic viability of peroxide consumption. This involves the preparation and maintenance costs of catalytic membranes, the loss of active components in the design of catalytic bed/tower structures, and the diverse characteristics of actual wastewater (such as pollutant types, pH fluctuations, and concentrations).

4. Properties of organics

Recent studies indicate that various reaction pathways, particularly non-radical oxidation systems, are preferred for targeted pollutant removal in complex environments. These systems exhibit intricate relationships with the electronic properties, hydrophilicity/hydrophobicity, and molecular structures of target organic compounds[95]. The inherent physicochemical properties of these organic substrates can influence system selectivity by modulating their affinity with catalysts, thereby exhibiting distinct reaction-dominant mechanisms (radical/non-radical pathways) and degradation kinetic characteristics (apparent rate constants). This leads to varying peroxide consumption rates and utilization of active substances. Therefore, deciphering the relationship between pollutant molecular characteristics and degradation behavior will facilitate the rational design of oxidation systems. This approach enables the achievement of system selectivity and high activity, thereby promoting the efficient utilization of peroxides.

4.1. Electronic properties

It was known that the non-radical active species (such as $^1O_2$, HVMs, and surface-bound complexes) offer significant advantages in enhancing peroxide utilization due to their high selectivity and resistance to environmental interference. However, the primary factors influencing this selective oxidation depend on the electronic properties of organic pollutants[207]. For instance, processes based on active intermediates and catalyst-mediated electron transfer demonstrate notable advantages in selectively removing electron-donating pollutants (e.g., phenolic compounds, aromatic amines). Conversely, electron-deficient pollutants (e.g., perfluoroalkyl substances, halogenated hydrocarbons) possess low electron density, making it difficult to trigger surface activation mechanisms. This results in a 'passivation effect' during oxidation (i.e., significantly reduced reaction activity), severely hindering the efficient utilization of peroxides[94, 208, 209]. Recently, to establish quantitative relationships between pollutant electronic properties and oxidation efficiency, a series of descriptors influencing pollutant oxidation fate —such as Hammett constant (σ), ionization potential (IP), energy of the highest occupied molecular orbital (E_{HOMO}), and half-wave potential ($\varphi_{1/2}$) — have been employed to develop quantitative structure-activity relationship (QSAR) models. These models aim to elucidate the fundamental mechanisms underlying selective oxidation via non-radical pathways.

Generally, organic pollutants containing electron-donat-

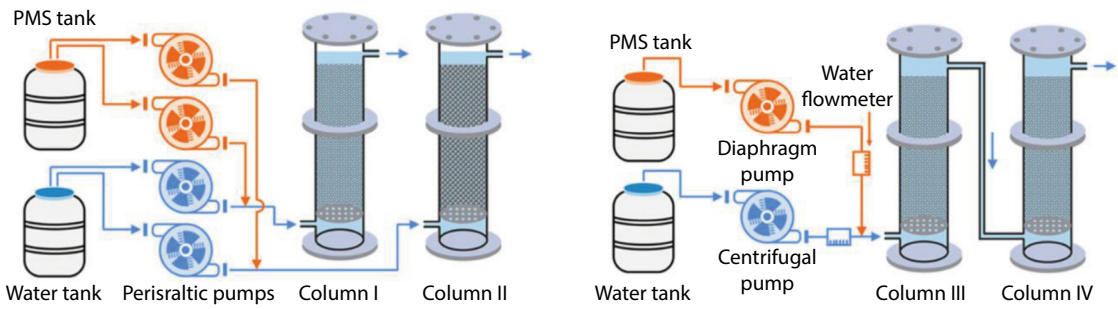

Fig. 7. Schematic illustration of the laboratory-scale and pilot-scale CuFeMnO-catalyzed PMS process. Reproduced with permission.[206] Copyright 2022, National Academy of Sciences.

ing groups (EDGs, such as -OH, -CH_3, -NH_2) react more readily with non-radicals than compounds bearing electron-withdrawing groups (EWGs, such as -COOH, -NO_2)[209, 210]. Therefore, this property is highly likely influenced by substituents. The Hammett constant, as a substituent descriptor, is commonly used to quantify the electron-donating or electron-withdrawing properties of substituents associated with aromatic compounds. Specifically, the sign (positive for electron-withdrawing groups, negative for electron-donating groups) and magnitude of the σ value quantitatively describe the electronic effect of the substituent[211, 212]. QSAR relationships have been established between the kinetic constants of phenolic pollutants with different substituents in various Fenton-type systems and their Hammett constants (σ, σ^+). Good linear correlations were observed in non-radical systems[213, 214], indicating that phenolic pollutants bearing electron-withdrawing groups (EDGs) degrade faster and exhibit a positive correlation with the number of EDGs. It should be noted that the applicability of this model is primarily limited to organic pollutants with aromatic main chains and substituents located at specific positions (meta or para), with limited applicability to complex structural pollutants.

Recent studies indicate that the theoretical descriptors ionization potential (IP) and energy of the highest occupied molecular orbital (E_{HOMO}) are also associated with selective oxidation characteristics. These descriptors serve as crucial parameters for evaluating the ability to donate or withdraw electrons and can be obtained through theoretical calculations on pollutants with known chemical structures[222, 223]. Consequently, researchers have proposed oxidation thresholds by establishing correlation models between these descriptors and apparent rate constants: pollutants can only be effectively oxidized when the IP value is below or the E_{HOMO} is above specific critical thresholds (Table 1). Thresholds exhibited across different oxidation systems show certain variations, potentially attributable to differences in the oxidation capacity of active species, reaction mechanisms, environmental conditions, and measurement methods. Notably, throughout the catalytic oxidation process, the oxidation pathways and mechanisms of organic pollutants are jointly determined by the catalyst and target pollutant. Therefore, modulating the interaction between organic pollutants and catalysts can effectively broaden the selective oxidation scope of non-radical pathways[224-226]. For instance, enhancing the adsorption effect between catalysts and organic pollutants offers a novel approach to address the low degradation efficiency of electron-deficient pollutants in non-radical pathways. Chen et al. constructed a Co-Mo bimetallic system by introducing Mo sites into a single-atom Co catalyst, enabling efficient degradation of organic pollutants with high ionization potential (IP) values through PMS activation[225]. The electron-donating effect of Mo sites on high-IP (>8.5 eV) pollutants effectively mitigates electron deficiency in electron-deficient contaminants, thereby promoting electron transfer. PMS activation efficiency increased nearly 20-fold compared to traditional Fenton-like systems, overcoming the selectivity limitations of non-radical systems for electron-deficient pollutant degradation. Furthermore, the efficiency of ETP is governed by the potential difference between the E_{HOMO} of the pollutant and the lowest unoccupied molecular orbital (E_{LUMO}) of the catalyst (or surface complex). Specifically, a smaller potential difference ($\Delta E = E_{LUMO} - E_{HOMO}$) is more conducive to ETP[94, 217, 221]. Therefore, for pollutants with lower E_{HOMO}, designing catalyst (or surface complex) systems with more negative E_{LUMO} can be attempted to narrow the energy gap and broaden the scope of ETP applicability.

The half-wave potential ($\varphi_{1/2}$) is considered to better reflect the reactivity of organic pollutants during non-radical oxidation processes and exhibits good linear correlation with IP and E_{HOMO} [227, 228]. However, this correlation holds only for simple organic compounds. To mitigate biases arising from pollutant complexity (e.g., spatial and polarity effects) and environmental factors (e.g., pH), Zhang et al. confirmed through multi-descriptor QSAR analysis that $\varphi_{1/2}$ is the dominant determinant of selective oxidation in carbon-based non-radical oxidation processes (C-NOPs). They established $\varphi_{1/2}$ as the benchmark for determining the oxidation threshold of C-NOPs (approximately 1.1 V vs SCE) [207]. Organic pollutants at oxidation potentials below this threshold undergo oxidation via electron extraction by active complexes. Furthermore, in systems where radical and non-radical mechanisms coexist, the electronic properties of pollutants influence the relative contributions of these mechanisms. For instance, in the M-SACs/PMS system, pollutants with low $\varphi_{1/2}$ (e.g., bisphenol A) are more susceptible to electron transfer control, resulting in nearly 100% ETP oxidation[221, 229]. In summary, adsorption affinity, the electronic properties of pollutants (such as electron-donating/electron-withdrawing groups), and redox potential collectively determine oxidation selectivity and peroxide utilization efficiency. Non-radical oxidation systems preferentially remove pollutants with lower electrophilic indices. These target pollutants typically exhibit faster reaction kinetics and a higher proportion of non-radical pathways, thereby promoting their directed activation pathways. This approach reduces

Table 1. Summary of oxidation thresholds of pollutants in different reaction systems: effective oxidation occurs when IP is below or E_{HOMO} is above specific critical values.

system	Main ROS/Oxidation pathways	IP Threshold(approximately)	E_{HOMO} Threshold(approximately)	References
K-FeOCl/H_2O_2	$Fe^{IV}=O$	8.40 eV	-	[215]
CPPy-F-8/PMS	Electronic transfer	9.00 eV	-	[216]
ZrO_2-C/PMS	PMS complexes	-	−6.52 eV	[217]
e-CuO@BC/PDS	$^1O_2$、PDS complexes	9.00 eV	-	[218]
Fe-NSC/PMS	$^1O_2$	9.00 eV	-	[219]
nCuO/PAA	$CH_3C(O)OO\cdot$	9.00 eV	-	[220]
M-SACs/PMS	Electronic transfer	-	−7.002 eV	[221]
PMS/Co_3O_4	$SO_4^{\cdot-}$	9.39 eV	-	[169]

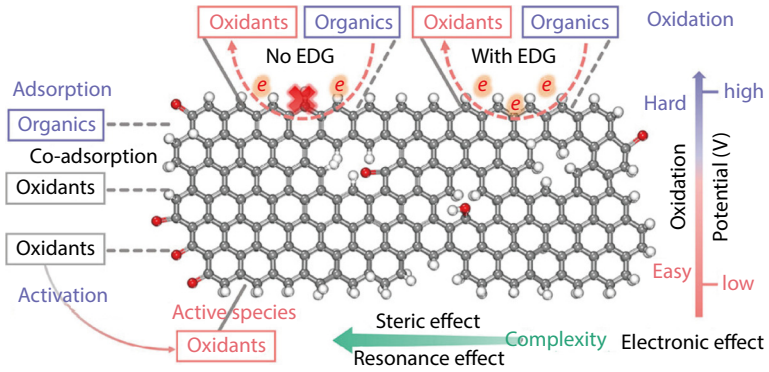

Scheme 1. Mechanism of Selective Oxidation in Carbon-Based Nonradical Oxidation Process. Reproduced with permission.[207] Copyright 2024, American Chemical Society.

the ineffective decomposition of peroxides and reactive species, ultimately lowering peroxide consumption. **Scheme 1** provides a typical mechanistic framework summarizing how pollutant characteristics —such as functional groups and half-wave potentials —govern non-radical oxidation pathways. Using carbon-based systems as an example, it demonstrates that adsorption affinity, the electronic properties of pollutants (e.g., electron-donating/electron-withdrawing groups), and redox potentials collectively determine oxidation selectivity and peroxide utilization. Consequently, non-radical oxidation systems preferentially remove pollutants with lower electrophilic indices. These target pollutants typically exhibit faster reaction kinetics and higher non-radical pathway contributions, thereby promoting their directed activation pathways. This approach reduces the ineffective decomposition of peroxides and reactive species, ultimately lowering peroxide consumption.

4.2. Additional characteristics

The inherent physicochemical properties of organic pollutants —such as molecular structure, molecular weight, hydrophobicity, and polarizability —can significantly modulate their interactions with catalyst surfaces, thereby influencing oxidation reaction pathways and catalytic efficiency[94, 230-232]. For instance, highly hydrophobic phenolic pollutants achieve selective enrichment on reduced graphene oxide (RGO) surfaces through the superhydrophobic properties of sp^2-hybridized carbon networks within graphite domains and strong π-π stacking interactions between the pollutant's benzene rings and the graphite lattice[233-235]. This interfacial enrichment enables rapid targeted degradation of pollutants by ROS (e.g., $^1O_2$ and radicals) generated at the interface, effectively circumventing ROS self-quenching due to mass transfer limitations and enhancing peroxide utilization efficiency. Furthermore, specific structural features of certain pollutants may play a critical role in their oxidation processes. Chen and colleagues, upon re-examining the classic iron oxide-based heterogeneous Fenton system, discovered that organic pollutants bearing carboxyl groups (e.g., benzoic acid and its derivatives) can trigger a preferential ETP oxidation mechanism. Specifically, the carboxyl group forms a specific complex with surface ≡Fe(III) sites, establishing a directed electron transfer pathway that facilitates electron transfer from the pollutant to H_2O_2[226]. In contrast, non-complexing pollutants degrade via diffusion-controlled hydroxyl radical pathways, a process susceptible to inhibition by radical quenchers, leading to higher H_2O_2 consumption. This mechanism enables selective oxidation of organics bearing functional ligand groups and can be extended to other pollutant structures capable of forming specific interactions with the catalyst.

Interestingly, in Fenton-like systems involving synergistic ROS interactions, it has been observed that certain ROS species may preferentially attack specific structural motifs within organic pollutants. This selective targeting enhances the effective reaction time (ERT) of ROS interacting with pollutants, thereby driving the oxidation of the target contaminant[236]. For instance, sulfate radicals prefer single-electron transfer (SET) reactions to directly attack unsaturated bonds or specific functional groups (e.g., -OH, $-NH_2$). However, their low steady-state concentration, short ERT, and weak attack on rigid aromatic rings limit their dominant role in practical systems[237-239]. In contrast, the electrophilic $^1O_2$ can directly oxidize electron-rich regions (e.g., sulfonyl or phenolic groups) via electrophilic attack. Fundamentally, $^1O_2$ often serves as the primary oxidant contributor when treating wastewater containing pollutants with these common or basic parent structures, despite its lower production rates and reaction rate constants compared to $HO^{\bullet}$ or $SO_4^{\bullet-}$[240, 241]. For pollutants containing saturated hydrocarbon chains or nitrogen-containing heterocyclic structures, $HO^{\bullet}$ contributes the highest oxidation efficiency due to its non-selective attack characteristics[236, 242]. Therefore, theoretical calculations can predict the dominant ROS species based on specific pollutant structural features, thereby guiding the design optimization of catalytic systems. This strategy enables the full utilization of ROS oxidation capabilities, thereby enhancing pollutant degradation efficiency and reducing peroxide consumption, providing a theoretical basis for rational wastewater treatment process design.

5. Concluding remarks and future perspectives

Fenton and Fenton-like systems have emerged as key AOPs for tackling recalcitrant organic pollutants. However, their practical application has long been hindered by high peroxide consumption and low utilization efficiency of reactive species. Recent discoveries indicate that utilizing non-radical species with higher selectivity and longer lifetimes—such as singlet oxygen, highly valent metal species, and surface-activated complexes—to oxidize various recalcitrant organic pollutants can significantly reduce peroxide consumption while maintaining high efficiency. Optimizing the physicochemical properties of

catalysts—such as morphology, pore structure, and conductivity —along with the local microenvironment of active sites (e.g., coordination, electron distribution, and pH) holds great promise for regulating non-radical pathways (transition from radical to non-radical mechanisms) and enabling the efficient generation and utilization of non-radical RS. Specifically, these precisely functionalized catalysts and integrated catalytic modules within reactors can overcome limitations of conventional catalysts (e.g., leaching of metal active species) while maximizing active site exposure for efficient peroxide activation. Furthermore, the inherent properties of organic pollutants —such as electronic characteristics, hydrophobicity, and molecular structure —significantly influence reaction mechanisms and kinetics. This underscores the necessity of tailoring oxidation strategies to pollutant specificity for achieving green economic systems. Collectively, these advances highlight the feasibility of ultra-low oxidant consumption systems while maintaining high degradation performance.

The strategies developed to reduce peroxide consumption must be applied to practical and large-scale water treatment, yet persistent challenges remain throughout this process. Efforts are focused on developing catalysts with high catalytic performance and selectivity through rational design of catalytic sites and structures. These catalysts demonstrate satisfactory mass transfer efficiency, zone dynamics, and stability, and crucially, achieve contaminant removal with ultra-low peroxide consumption. However, the trend toward more sophisticated and complex materials has resulted in intricate procedures and high costs that hinder their deployment in practical applications. It is therefore essential to integrate techno-economic assessment (TEA) and life-cycle analysis (LCA) frameworks in future investigations to bridge the gap between laboratory innovation and engineering practice. Material synthesis and characterization should better align with application budgets and requirements. Recent examples demonstrating the conversion of agricultural/industrial wastes (e.g., fly ash, livestock manure, spent catalysts) into high-performance Fenton-like catalysts via simple processes have proven the feasibility of waste resource utilization alongside zero-discharge and zero-pollution objectives. Standardization and quality control of these waste-derived catalysts are crucial for ensuring reproducibility and long-term stability, thereby addressing engineering bottlenecks in catalyst recycling and operational reliability.[130]. We believe this represents a priority direction for future sustainable development and practical implementation. It is imperative to emphasize that waste-derived catalysts require rigorous standardization to ensure consistent performance and mitigate the risk of deactivation induced by impurities. Furthermore, computational simulations can be combined with experimental validation to guide the design of Fenton and Fenton-like catalysts with low peroxide consumption. DFT calculations can reveal how catalyst structures influence radical and non-radical pathways, while molecular dynamics simulations can model dynamic surface interactions under real-world conditions. Integrating these computational results with experimental data —including catalyst structures, pollutant properties, and peroxide consumption—enables machine learning to predict optimal catalyst configurations and reaction conditions, providing a viable framework for efficient and highly selective oxidation processes.

Although various strategies to reduce peroxide consumption have been identified in Fenton and Fenton-like systems, numerous challenges remain until the relationship between peroxides, catalysts, and pollutants is fully understood. Throughout the reaction process, the removal capacity of organic pollutants and peroxide consumption result from the combined effects of catalyst performance, peroxide selection, target pollutant properties, and various reaction conditions. Optimizing a single parameter may yield suboptimal results. Currently, the impact of peroxide variations on adsorption and activation processes during selective oxidation has not been systematically investigated, and uncertainties persist regarding the oxidation mechanisms for novel and more complex pollutants. Therefore, establishing this structure-reactivity relationship is essential to bridge the significant gap between limited experimental data and the ever-increasing number of anthropogenic pollutants. This will aid in selecting appropriate AOPs to achieve cost-effective peroxide utilization.

At present, introducing external energy fields to enhance the reactivity of Fenton and Fenton-like systems has become a widely applied intensification strategy. Various forms of energy, such as light, heat, ultrasound, and electricity, can effectively promote the activation of peroxides and accelerate reaction rates, thereby significantly improving the degradation efficiency of the system[243-245]. However, such energy-driven processes are inevitably accompanied by additional energy consumption, and improper parameter settings may even lead to adverse effects —for instance, excessive energy input can induce the non-selective and rapid decomposition of peroxides, resulting in the waste of reactive species and a decline in overall efficiency. Therefore, it is essential to optimize reaction conditions and energy input parameters from the perspective of energy efficiency, and to explore the synergistic effects of multiple energy forms, so as to achieve an optimal balance between reaction performance and energy consumption, ultimately realizing the dual minimization of energy utilization and peroxide consumption.

Acknowledgments

This research was funded by the Sichuan Science and Technology Program (grant 2023NSFSC0801), the Chongqing Municipal Education Commission (grants KJZD-K202500201, KJQN202200202 and KJQN202100214), and the Natural Science Foundation of Chongqing (grant CSTB2022NSCQ-MSX0448).

Conflicts of Interest

The authors declare no competing interests.

References

[1] Shanmugavel, S. P.; Kumar, G.; Yogalakshmi K, N.; Gunasekaran, M.; Rajesh Banu, J. Recent progress in mineralization of emerging contaminants by advanced oxidation process: A review. *Environ. Pollut.*, 2024, 341: 122842.

[2] Guo, J.; Tu, K.; Chou, L. B.; Zhang, Y.; Wei, S.; Zhang, X. W.; Yu, H. X.; Shi, W. Deep mining of reported emerging contaminants in China's surface water in the past decade: Exposure, ecological effects and risk assessment. *Water Res.*, 2023, 243: 120318.

[3] Rojas, S.; Horcajada, P. Metal–organic frameworks for the removal of emerging organic contaminants in water. *Chem. Rev.*,

2020, 120(16): 8378–8415.

[4] Qian, J. S.; Zhang, X.; Jia, Y. Q.; Xu, H.; Pan, B. C. Oxidative polymerization in water treatment: Chemical fundamentals and future perspectives. *Environ. Sci. Technol.*, 2025, 59(2): 1060–1079.

[5] Huang, J. T.; Sharif, H. M. A.; Mahmood, A.; Li, C. P. Unveiling the heterojunction of Fe_3O_4@MXene nanocatalyst for ultrafast degradation of antibiotics *via* non-radical pathway. *Chem. Eng. J.*, 2024, 500: 156941.

[6] Lin, L.; Wang, J. S.; Zhao, Z. F.; Zhu, J. Y.; Zhamaerding, A.; Feng, L. Y.; Yang, D.; Meng, L. T.; He, C. S.; Wang, W. B. et al. Multi-dimensional micro-nano scale manganese oxide catalysts induced chemical-based advanced oxidation processes (AOPs) in environmental applications: A critical review. *Chem. Eng. J.*, 2023, 474: 145600.

[7] Du, Z. L.; Zhu, C. Q.; Jing, S. C.; Yue, C. L.; Liu, F. Q.; Li, A. M. Boosting dissolved oxygen utilization by oriented electron transfer on dual-site S-scheme heterojunction for low-H_2O_2-consumption photo-Fenton reaction. *Chem. Eng. J.*, 2023, 462: 142146.

[8] Ao, X. W.; Eloranta, J.; Huang, C. H.; Santoro, D.; Sun, W. J.; Lu, Z. D.; Li, C. Peracetic acid-based advanced oxidation processes for decontamination and disinfection of water: A review. *Water Res.*, 2021, 188: 116479.

[9] Yang, Y.; Pignatello, J. J.; Ma, J.; Mitch, W. A. Comparison of halide impacts on the efficiency of contaminant degradation by sulfate and hydroxyl radical-based advanced oxidation processes (AOPs). *Environ. Sci. Technol.*, 2014, 48(4): 2344–2351.

[10] Li, J.; Yang, T.; Zeng, G.; An, L. Q.; Jiang, J.; Ao, Z. M.; Ma, J. Ozone- and hydroxyl radical-induced degradation of micropollutants in a novel UVA-LED-activated periodate advanced oxidation process. *Environ. Sci. Technol.*, 2023, 57(47): 18607–18616.

[11] Wang, F.; Dong, W. Y.; Zhao, Z. L.; Wang, H. J.; Li, W. T.; Zhang, L.; Ouyang, H.; Huang, X.; Li, J. Mechanistic insights into Fe(II)-citric acid complex catalyzed CaO_2 Fenton-like process for enhanced benzo [a] pyrene removal from black-odor sediment at circumneutral pH. *Water Res.*, 2022, 226: 119233.

[12] Zhang, S. N.; Hao, Z. N.; Liu, J. F.; Gutierrez, L.; Croué, J. P. Molecular insights into the reactivity of aquatic natural organic matter towards hydroxyl ($^{\bullet}OH$) and sulfate ($SO_4^{\bullet-}$) radicals using FT-ICR MS. *Chem. Eng. J.*, 2021, 425: 130622.

[13] Huang, Y.; Jiang, M. L.; Gao, S. M.; Wang, W.; Liu, Z. J.; Yuan, R. X. Non-radical pathway dominated by singlet oxygen under high salinity condition towards efficient degradation of organic pollutants and inhibition of AOX formation. *Sep. Purif. Technol.*, 2022, 291: 120921.

[14] Han, Y. F.; Zhao, C. F.; Zhang, W. C.; Liu, Z.; Li, Z.; Han, F.; Zhang, M. R.; Xu, F.; Zhou, W. Z. Cu-doped CoOOH activates peroxymonosulfate to generate high-valent cobalt-oxo species to degrade organic pollutants in saline environments. *Appl. Catal. B Environ.*, 2024, 340: 123224.

[15] Yang, Z. Z.; Zhou, Z. Y.; Tan, X. F.; Zeng, G. M.; Zhang, C. MXene-induced electronic structure modulation of Fe-Al-LDH to boost the Fenton-like Reaction: Singlet oxygen evolution and electron-transfer mechanisms. *J. Mater. Sci. Technol.*, 2025, 204: 224–237.

[16] Yang, Z. C.; Qian, J. S.; Shan, C.; Li, H. C.; Yin, Y. Y.; Pan, B. C. Toward selective oxidation of contaminants in aqueous systems. *Environ. Sci. Technol.*, 2021, 55(21): 14494–14514.

[17] Dong, N. N.; Ge, L. F.; Chen, P.; Wang, W.; Tan, F. T.; Wang, X. Y.; Qiao, X. L.; Wong, P. K. Non-radical activation of CaO_2 nanoparticles by MgNCN/MgO composites for efficient remediation of organic and heavy metal-contaminated wastewater. *Sep. Purif. Technol.*, 2022, 285: 120334.

[18] Yu, D. H.; He, J. G.; Bai, L. M.; Zheng, Y. S.; Wang, Z. Y.; Lefebvre, O.; Zhang, J. High-valent metal-oxo species heterogeneous activation making use of MoS_2 in a novel Electro-Fenton System: pH-independent catalytic environment and nonradical generation mechanism. *Chem. Eng. J.*, 2024, 479: 147573.

[19] Song, Z.; Zhang, Y.; Yang, Y. H.; Chen, Y. D.; Ren, N. Q.; Duan, X. G. Kinetics and mechanisms of non-radically and radically induced degradation of bisphenol A in a peroxymonosulfate-chloride system. *Environ. Sci. Ecotechnol.*, 2024, 22: 100452.

[20] Zhan, G. W.; Zeng, H. C. Charge-switchable integrated nanocatalysts for substrate-selective degradation in advanced oxidation processes. *Chem. Mater.*, 2016, 28(13): 4572–4582.

[21] Zeng, Y. F.; He, D. Q.; Sun, J. Q.; Zhang, A. P.; Luo, H. W.; Pan, X. L. Non-radical oxidation driven by iron-based materials without energy assistance in wastewater treatment. *Water Res.*, 2024, 264: 122255.

[22] Zhang, P. P.; Yang, Y. Y.; Duan, X. G.; Wang, S. B. Oxidative polymerization *versus* degradation of organic pollutants in heterogeneous catalytic persulfate chemistry. *Water Res.*, 2024, 255: 121485.

[23] Wang, L. J.; Xiao, K.; Zhao, H. Z. The debatable role of singlet oxygen in persulfate-based advanced oxidation processes. *Water Res.*, 2023, 235: 119925.

[24] Al-Nu'airat, J.; Dlugogorski, B. Z.; Gao, X. P.; Zeinali, N.; Skut, J.; Westmoreland, P. R.; Oluwoye, I.; Altarawneh, M. Reaction of phenol with singlet oxygen. *Phys. Chem. Chem. Phys.*, 2019, 21: 171–183.

[25] Hong, P. D.; Wu, Z. J.; Yang, D. D.; Zhang, K. S.; He, J. Y.; Li, Y. L.; Xie, C.; Yang, W.; Yang, Y.; Kong, L. T. et al. Efficient generation of singlet oxygen ($^1O_2$) by hollow amorphous Co/C composites for selective degradation of oxytetracycline *via* Fenton-like process. *Chem. Eng. J.*, 2021, 421: 129594.

[26] Xie, Z. H.; He, C. S.; Pei, D. N.; Dong, Y. D.; Yang, S. R.; Xiong, Z. K.; Zhou, P.; Pan, Z. C.; Yao, G.; Lai, B. Review of characteristics, generation pathways and detection methods of singlet oxygen generated in advanced oxidation processes (AOPs). *Chem. Eng. J.*, 2023, 468: 143778.

[27] Zhang, S.; Sun, M.; Hedtke, T.; Deshmukh, A.; Zhou, X. C.; Weon, S.; Elimelech, M.; Kim, J. H. Mechanism of heterogeneous Fenton reaction kinetics enhancement under nanoscale spatial confinement. *Environ. Sci. Technol.*, 2020, 54: 10868–10875.

[28] Wang, Y.; Lin, Y.; He, S. Y.; Wu, S. H.; Yang, C. P. Singlet oxygen: Properties, generation, detection, and environmental applications. *J. Hazard. Mater.*, 2024, 461: 132538.

[29] Bu, Y. G.; Li, H. C.; Yu, W. J.; Pan, Y. F.; Li, L. J.; Wang, Y. F.; Pu, L. T.; Ding, J.; Gao, G. D.; Pan, B. C. Peroxydisulfate activation and singlet oxygen generation by oxygen vacancy for degradation of contaminants. *Environ. Sci. Technol.*, 2021, 55(3): 2110–2120.

[30] Gao, Y. W.; Li, T.; Zhu, Y.; Chen, Z. H.; Liang, J. Y.; Zeng, Q. Y.; Lyu, L.; Hu, C. Highly nitrogen-doped porous carbon transformed from graphitic carbon nitride for efficient metal-free catalysis. *J. Hazard. Mater.*, 2020, 393: 121280.

[31] Nidheesh, P. V.; Boczkaj, G.; Ganiyu, S. O.; Oladipo, A. A.; Fedorov, K.; Xiao, R. Y.; Dionysiou, D. D. Generation, properties, and applications of singlet oxygen for wastewater treatment: A review. *Environ. Chem. Lett.*, 2025, 23: 195–240.

[32] Yi, Q. Y.; Li, Y.; Dai, R. B.; Li, X. S.; Li, Z. Y.; Wang, Z. W. Efficient removal of neonicotinoid by singlet oxygen dominated MoS_x/ceramic membrane-integrated Fenton-like process. *J. Hazard. Mater.*, 2022, 439: 129672.

[33] Yang, Z. C.; Qian, J. S.; Yu, A. Q.; Pan, B. C. Singlet oxygen mediated iron-based Fenton-like catalysis under nanoconfinement. *Proc. Natl. Acad. Sci. U. S. A.*, 2019, 116: 6659–6664.

[34] Huang, B. C.; Jiang, J.; Huang, G. X.; Yu, H. Q. Sludge biochar-based catalysts for improved pollutant degradation by activating peroxymonosulfate. *J. Mater. Chem. A*, 2018, 6: 8978–8985.

[35] Liang, P.; Zhang, C.; Duan, X. G.; Sun, H. Q.; Liu, S. M.; Tade, M. O.; Wang, S. B. N-doped graphene from metal–organic frameworks

for catalytic oxidation of p-hydroxylbenzoic acid: N-functionality and mechanism. *ACS Sustainable Chem. Eng.*, 2017, *5*(3), 2693–2701.

[36] Zhou, X. Q.; Zhao, Q. D.; Wang, J.; Chen, Z. L.; Chen, Z. Q. Nonradical oxidation processes in PMS-based heterogeneous catalytic system: Generation, identification, oxidation characteristics, challenges response and application prospects. *Chem. Eng. J.*, 2021, 410: 128312.

[37] Fukuzumi, S.; Kojima, T.; Lee, Y. M.; Nam, W. High-valent metal-oxo complexes generated in catalytic oxidation reactions using water as an oxygen source. *Coord. Chem. Rev.*, 2017, 333: 44–56.

[38] Kang, H.; Lee, D.; Lee, K. M.; Kim, H. H.; Lee, H.; Kim, M. S.; Lee, C. H. Nonradical activation of peroxymonosulfate by hematite for oxidation of organic compounds: A novel mechanism involving high-valent iron species. *Chem. Eng. J.*, 2021, 426: 130743.

[39] Dong, H. Y.; Li, Y.; Wang, S. C.; Liu, W. F.; Zhou, G. M.; Xie, Y. F.; Guan, X. H. Both Fe(IV) and radicals are active oxidants in the Fe(II)/peroxydisulfate process. *Environ. Sci. Technol. Lett.*, 2020, 7(3): 219–224.

[40] Pan, L. H.; Shi, W.; Sen, T.; Wang, L. Z.; Zhang, J. L. Visible light-driven selective organic degradation by $FeTiO_3$/persulfate system: The formation and effect of high valent Fe(IV). *Appl. Catal. B Environ.*, 2021, 280: 119414.

[41] Miao, J.; Song, J.; Lang, J. Y.; Zhu, Y.; Dai, J.; Wei, Y.; Long, M. C.; Shao, Z. P.; Zhou, B. X.; Alvarez, P. J. J. et al. Single-atom MnN5 catalytic sites enable efficient peroxymonosulfate activation by forming highly reactive Mn(IV)–oxo species. *Environ. Sci. Technol.*, 2023, 57(10): 4266–4275.

[42] Zong, Y.; Shao, Y. F.; Zeng, Y. Q.; Shao, B. B.; Xu, L. Q.; Zhao, Z. Y.; Liu, W.; Wu, D. L. Enhanced oxidation of organic contaminants by iron(II)-activated periodate: The significance of high-valent iron–oxo species. *Environ. Sci. Technol.*, 2021, 55: 7634–7642.

[43] Wang, Q.; Liu, C.; Zhou, D. M.; Chen, X. R.; Zhang, M.; Lin, K. F. Degradation of bisphenol A using peroxymonosulfate activated by single-atomic cobalt catalysts: Different reactive species at acidic and alkaline pH. *Chem. Eng. J.*, 2022, 439: 135002.

[44] Hu, Y. Y.; Sun, S. Y.; Guo, J. L.; Cheng, F.; Li, Z. K. *In situ* anchoring strategy to enhance dual nonradical degradation of sulfamethoxazole with high loading manganese doped carbon nitride. *Chemosphere*, 2022, *303*, 135035.

[45] Gao, X.; Li, J. N.; Chen, J.; Che, H. N.; Wang, P. F.; Liu, B.; Ao, Y. H. New insight into the mechanism of symmetry-breaking charge separation induced high-valent iron(IV) for highly efficient photodegradation of organic pollutants. *Appl. Catal. B Environ.*, 2023, 321: 122066.

[46] Yu, Y. H.; Dong, H. Y.; Lian, L. S.; Guan, X. H. Selective and rapid degradation of organic contaminants by Mn(V) generated in the Mn(II)-nitrilotriacetic acid/periodate process. *Chem. Eng. J.*, 2022, 443: 136387.

[47] Li, S.; Yang, Y. L.; Niu, J. F.; Zheng, H. S.; Zhang, W.; Leong, Y. K.; Chang, J. S.; Lai, B. Activation of PAA at the Fe–nx sites by boron nitride quantum dots enhanced charge transfer generates high-valent metal-oxo species for antibiotics degradation. *Environ. Sci. Technol.*, 2024, 58(49): 21871–21881.

[48] Liu, B. H.; Guo, W. Q.; Jia, W. R.; Wang, H. Z.; Si, Q. S.; Zhao, Q.; Luo, H. C.; Jiang, J.; Ren, N. Q. Novel nonradical oxidation of sulfonamide antibiotics with co(II)-doped g-C_3N_4-activated peracetic acid: Role of high-valent cobalt–oxo species. *Environ. Sci. Technol.*, 2021, 55: 12640–12651.

[49] Guo, M.; Lee, Y. M.; Fukuzumi, S.; Nam, W. Biomimetic metal-oxidant adducts as active oxidants in oxidation reactions. *Coord. Chem. Rev.*, 2021, 435: 213807.

[50] Yang, B. W.; Liu, H. T.; Zhang, J. High-valent metals in advanced oxidation processes: A critical review of their identification methods, formation mechanisms, and reactivity performance. *Chem. Eng. J.*, 2023, 460: 141796.

[51] Pan, Q. Y.; Wang, C. Q.; Zhan, P.; Zhao, F. F.; Dai, H. L.; Hu, Y. Y.; Hu, F. P.; Peng, X. M. Generation and regulation of high-valent metal species in advanced oxidation processes. *Environ. Funct. Mater.*, 2025

[52] Li, W. B.; Tang, R. D.; Xiong, S.; Li, L.; Zhou, Z. P.; Su, L.; Gong, D. X.; Deng, Y. C. High-valent metal-oxo species in catalytic oxidations for environmental remediation and energy conversion. *Coord. Chem. Rev.*, 2024, 510: 215840.

[53] Kim, H. H.; Lee, H.; Lee, D.; Ko, Y. J.; Woo, H.; Lee, J.; Lee, C. H.; Pham, A. L. Activation of hydrogen peroxide by a titanium oxide-supported iron catalyst: Evidence for surface Fe(IV) and its selectivity. *Environ. Sci. Technol.*, 2020, 54(23): 15424–15432.

[54] He, Z. H.; Wang, W. L.; Li, B.; Liu, C. MoS_2-assisted iron-driven peroxydisulfate activation for green and sustainable water purification. *Green Chem.*, 2025.

[55] Li, A.; Li, B.; Sun, L. M.; Liu, L. X.; Liu, C.; Dong, Y. M.; Zhang, X. High valent manganese-oxo species activation of peroxymonosulfate by different phases manganese oxides nanoplates for catalytic water decontamination. *Chem. Eng. J.*, 2024, 496: 154135.

[56] Yu, J. X.; Gong, Z. Y.; Wang, S. H.; Zhong, H. J.; Tao, Y.; Hou, Y.; Fu, Q.; Yang, H. S.; Li, J. Q.; Wang, J. H. et al. Two major deactivation mechanisms in carbon-based advanced oxidation processes (AOPs) dominated by electron-transfer pathway (ETP). *Appl. Catal. B Environ. Energy*, 2025, 364: 124850.

[57] Wu, B.; Li, Z. L.; Zu, Y. X.; Lai, B.; Wang, A. J. Polar electric field-modulated peroxymonosulfate selective activation for removal of organic contaminants *via* non-radical electron transfer process. *Water Res.*, 2023, 246: 120678.

[58] Li, S.; Dai, C. M.; Wan, L. C.; Li, J. X.; Duan, Y. P.; You, X. J.; Yang, S. L.; Hu, J. J.; Guo, J. F.; Zhang, Y. L. et al. Unveiling the role of groundwater matrices in electron transfer efficiency of peracetic acid-based advanced oxidation processes. *Sep. Purif. Technol.*, 2025, 361: 131564.

[59] Zhao, X. Y.; Zhang, Z. H. Heterogeneous peroxymonosulfate-based advanced oxidation mechanisms: New wine in old bottles. *Environ. Sci. Technol.*, 2025, 59(12): 5913–5924.

[60] Lian, T. T.; Wang, Y.; Wu, B. L.; Yang, F.; Tarakina, N. V.; Antonietti, M. 'Green-to-Green': Iron oxides embedded in lignin-based carbon scaffolds for water remediation *via* oxidation excluding free-radical pathways. *J. Hazard. Mater.*, 2023, 442: 130070.

[61] Ren, W.; Cheng, C.; Shao, P. H.; Luo, X. B.; Zhang, H.; Wang, S. B.; Duan, X. G. Origins of electron-transfer regime in persulfate-based nonradical oxidation processes. *Environ. Sci. Technol.*, 2022, 56(1): 78–97.

[62] Zeng, G. S.; Yang, Y. L.; Li, D. X.; Kuang, C. Z.; Wang, R. Y.; Zhong, J. P.; Tian, F. H.; Guo, W.; Li, C. H. Enhanced peroxymonosulfate activation by δ-MnO_2 nanocatalyst enriched with oxygen vacancies for phenolic pollutants polymerization. *Appl. Catal. B Environ. Energy*, 2024, 357: 124327.

[63] Liu, T. Y.; Wang, C.; Han, Y. Z.; Bai, C.; Ren, H. T.; Liu, Y.; Han, X. Oxidative polymerization of bisphenol A (BPA) *via* H-abstraction by $Bi_{2.15}WO_6$ and persulfate: Importance of the surface complexes. *Chem. Eng. J.*, 2022, 435: 134816.

[64] Jiang, Y. Q.; Yang, Z. H.; Bi, X. R.; Yao, N.; Zhao, P. Q.; Meng, X. Mediated electron transfer process in α-MnO_2 catalyzed Fenton-like reaction for oxytetracycline degradation. *Chin. Chem. Lett.*, 2024, 35: 109331.

[65] Chen, C. C.; Zhao, M. Y.; Chen, Y. H.; Jia, W. R.; Wu, Y. H.; Liang, Y. Q.; Du, J. S.; Wu, Q. L.; Feng, X. C.; Wang, H. Z. et al. Constructing nanoconfined spaces in persulfate oxidation processes for efficient degradation of emerging contaminants: Structures, mechanisms, and challenges. *Sep. Purif. Technol.*, 2025, 354: 128689.

[66] Ren, W.; Nie, G.; Zhou, P.; Zhang, H.; Duan, X. G.; Wang, S. B. The intrinsic nature of persulfate activation and N-doping in carbocatalysis. *Environ. Sci. Technol.*, 2020, 54(10): 6438–6447.

[67] Wang, J.; Lv, H.; Tong, X. D.; Ren, W.; Shen, Y.; Lu, L.; Zhang, Y. Modulation of radical and nonradical pathways *via* modified carbon nanotubes toward efficient oxidation of binary pollutants in water. *J. Hazard. Mater.*, 2023, 459: 132334.

[68] Liu, B. H.; Guo, W. Q.; Wang, H. Z.; Zheng, S. S.; Si, Q. S.; Zhao, Q.; Luo, H. C.; Ren, N. Q. Peroxymonosulfate activation by cobalt(II) for degradation of organic contaminants *via* high-valent cobalt-oxo and radical species. *J. Hazard. Mater.*, 2021, 416: 125679.

[69] Zhang, R. Y.; Zheng, X. X.; Chen, B. H.; Ma, J. L.; Niu, X. J.; Zhang, D. Q.; Lin, Z.; Fu, M. L.; Zhou, S. Q. Enhanced adsorption of sulfamethoxazole from aqueous solution by Fe-impregnated graphited biochar. *J. Clean. Prod.*, 2020, 256: 120662.

[70] Luo, C. W.; Ma, J.; Jiang, J.; Liu, Y. Z.; Song, Y.; Yang, Y.; Guan, Y. H.; Wu, D. J. Simulation and comparative study on the oxidation kinetics of atrazine by UV/H_2O_2, UV/HSO5−. *Water Res.*, 2015, 80: 99–108.

[71] Huo, Y. P.; Zheng, H. Y.; Jiang, Y. Y.; Chen, H. H.; Cao, W. M.; Mameda, N.; Nghiem, L. D.; Zhang, X. L.; Liu, Q. Comparison and characterization of nitrogen/sulfur-doped activated carbon for activating peroxydisulfate to degrade acid orange 7: An experimental and theoretical study. *Ind. Eng. Chem. Res.*, 2023, 62(30): 11894–11904.

[72] Qiu, X. J.; Zhao, Y. X.; Li, C. X.; Jin, R. T.; Mutabazi, E. Different peroxymonosulfate activation and utilization pathways of typical cobalt oxides, cobalt-carbon and carbonaceous composites derived from metal-organic frameworks for pollutant oxidation in wastewater. *Chem. Eng. J.*, 2023, 475: 146234.

[73] Ahn, Y. Y.; Bae, H.; Kim, H. I.; Kim, S. H.; Kim, J. H.; Lee, S. G.; Lee, J. Surface-loaded metal nanoparticles for peroxymonosulfate activation: Efficiency and mechanism reconnaissance. *Appl. Catal. B Environ.*, 2019, 241: 561–569.

[74] Khan, J. A.; He, X. X.; Shah, N. S.; Khan, H. M.; Hapeshi, E.; Fatta-Kassinos, D.; Dionysiou, D. D. Kinetic and mechanism investigation on the photochemical degradation of atrazine with activated H_2O_2, $S_2O_8^{2-}$ and HSO_5^-. *Chem. Eng. J.*, 2014, 252: 393–403.

[75] Zhan, H. Y.; Zhou, R. R.; Wang, P. F.; Zhou, Q. X. Selective hydroxyl generation for efficient pollutant degradation by electronic structure modulation at Fe sites. *Proc. Natl. Acad. Sci. USA*, 2023, 120: e2305378120.

[76] Shan, C.; Liu, Y.; Huang, Y. H.; Pan, B. C. Non-radical pathway dominated catalytic oxidation of As(III) with stoichiometric H_2O_2 over nanoceria. *Environ. Int.*, 2019, 124: 393–399.

[77] Hong, P. D.; Zhang, K. S.; He, J. Y.; Li, Y. L.; Wu, Z. J.; Xie, C.; Liu, J. H.; Kong, L. T. Selenization governs the intrinsic activity of copper-cobalt complexes for enhanced non-radical Fenton-like oxidation toward organic contaminants. *J. Hazard. Mater.*, 2022, 435: 128958.

[78] Kim, D. H.; Bokare, A. D.; Koo, M. S.; Choi, W. Heterogeneous catalytic oxidation of As(III) on nonferrous metal oxides in the presence of H_2O_2. *Environ. Sci. Technol.*, 2015, 49(6): 3506–3513.

[79] Parvulescu, V. I.; Epron, F.; Garcia, H.; Granger, P. Recent progress and prospects in catalytic water treatment. *Chem. Rev.*, 2022, 122(3): 2981–3121.

[80] Ma, W. J.; Ren, X. H.; Li, J. H.; Wang, S.; Wei, X. Y.; Wang, N.; Du, Y. C. Advances in atomically dispersed metal and nitrogen Co-doped carbon catalysts for advanced oxidation technologies and water remediation: From microenvironment modulation to non-radical mechanisms. *Small*, 2024, 20: 2308957.

[81] Wang, Z. W.; Wang, W. L.; Wang, J.; Yuan, Y.; Wu, Q. Y.; Hu, H. Y. High-valent iron-oxo species mediated cyclic oxidation through single-atom Fe-N_6 sites with high peroxymonosulfate utilization rate. *Appl. Catal. B Environ.*, 2022, 305: 121049.

[82] Luo, R.; Li, M. Q.; Wang, C. H.; Zhang, M.; Nasir Khan, M. A.; Sun, X. Y.; Shen, J. Y.; Han, W. Q.; Wang, L. J.; Li, J. S. Singlet oxygen-dominated non-radical oxidation process for efficient degradation of bisphenol A under high salinity condition. *Water Res.*, 2019, 148: 416–424.

[83] Zhang, T.; Chen, Y.; Wang, Y. R.; Le Roux, J.; Yang, Y.; Croué, J. P. Efficient peroxydisulfate activation process not relying on sulfate radical generation for water pollutant degradation. *Environ. Sci. Technol.*, 2014, 48(10): 5868–5875.

[84] Shi, K. G.; Parsons, Z. S.; Feng, X. F. Sensitivity of gas-evolving electrocatalysis to the catalyst microenvironment. *ACS Energy Lett.*, 2023, 8(7): 2919–2926.

[85] Liu, Z. Y.; Wang, L. M.; Wang, C. G.; Li, R. S.; Zhou, P. Y.; Gao, H. Y.; Wang, G. Modulating the strong metal-support interactions by regulating the chemical microenvironment of Pt confined in MOFs for low temperature hydrogenation of DCPD. *Chem. Eng. J.*, 2024, 479: 147601.

[86] Chen, F.; Sun, Y. J.; Huang, X. T.; Bai, C. W.; Zhang, Z. Q.; Duan, P. J.; Chen, X. J.; Yang, Q.; Yu, H. Q. Embedding electronic perpetual motion into single-atom catalysts for persistent Fenton-like reactions. *Proc. Natl. Acad. Sci. USA*, 2024, 121: e2314396121.

[87] Zhu, Z. S.; Zhong, S.; Cheng, C.; Zhou, H. Y.; Sun, H. Q.; Duan, X. G.; Wang, S. B. Microenvironment engineering of heterogeneous catalysts for liquid-phase environmental catalysis. *Chem. Rev.*, 2024, 124(20): 11348–11434.

[88] Wang, Y. Z.; Zhong, M. X.; Ma, F. Q.; Wang, C.; Lu, X. F. Shell-induced enhancement of Fenton-like catalytic performance towards advanced oxidation processes: Concept, mechanism, and properties. *Water Res.*, 2025, 268: 122655.

[89] Qiu, W. Q.; Cui, J. L.; Zhu, K. J.; Gao, M.; Zheng, X. H.; Liu, H.; Guo, Z. X.; Zhang, Z. X.; Zhao, Y. J. Microenvironment effect catalysis with phosphoric acid-based covalent organic frameworks. *ACS Catal.*, 2024, 14(19): 14780–14786.

[90] Sheng, X. D.; Ge, W. X.; Jiang, X. L.; Jiang, H. L.; Zhu, D. L.; Fu, L. C.; Li, C. Z. Engineering catalytic microenvironment enabling direct carbonate electrolysis to ethylene. *Ind. Eng. Chem. Res.*, 2024, 63(43): 18371–18379.

[91] Zhou, X.; Ke, M. K.; Huang, G. X.; Chen, C.; Chen, W. X.; Liang, K.; Qu, Y. T.; Yang, J.; Wang, Y.; Li, F. T. et al. Identification of Fenton-like active Cu sites by heteroatom modulation of electronic density. *Proc. Natl. Acad. Sci. USA*, 2022, 119: e2119492119.

[92] Li, B.; Cheng, X. L.; Zou, R. S.; Yong, X. Y.; Pang, C. F.; Su, Y. Y.; Zhang, Y. F. Simple modulation of Fe-based single atoms/clusters catalyst with acidic microenvironment for ultrafast Fenton-like reaction. *Appl. Catal. B Environ.*, 2022, 304: 121009.

[93] Sun, T.; Mitchell, S.; Li, J.; Lyu, P.; Wu, X. B.; Pérez-Ramírez, J.; Lu, J. Design of local atomic environments in single-atom electrocatalysts for renewable energy conversions. *Adv. Mater.*, 2021, 33: 2003075.

[94] Li, S. Y.; Wang, J.; Ye, Y. Y.; Tang, Y. M.; Li, X. K.; Gu, F. L.; Li, L. S. Composite Si-O-metal network catalysts with uneven electron distribution: Enhanced activity and electron transfer for catalytic ozonation of carbamazepine. *Appl. Catal. B Environ.*, 2020, 263: 118311.

[95] Luo, M. F.; Zhang, H.; Zhao, J.; Liu, Y.; Xiong, Z. K.; Du, Y.; Lai, B. Interfacial catalysis of peroxides for water decontamination: A critical review on fundamental origins and selective oxidation. *Chem. Eng. J.*, 2024, 488: 151156.

[96] Wang, B.; Chen, Y. F.; Liu, G.; Liu, D. W.; Liu, Y. F.; Ge, C. Q.; Wang, L.; Wang, Z. G.; Wu, R. B.; Wang, L. Y. Interfaces coupling of Co_8FeS_8-Fe_5C_2 with elevated d-band center for efficient water oxidation catalysis. *Appl. Catal. B Environ.*, 2024, 341: 123294.

[97] Zhang, L. S.; Jiang, X. H.; Zhong, Z. A.; Tian, L.; Sun, Q.; Cui, Y. T.; Lu, X.; Zou, J. P.; Luo, S. L. Carbon nitride supported high-loading Fe single-atom catalyst for activation of peroxymonosulfate

to generate $^1O_2$ with 100% selectivity. *Angew. Chem. Int. Ed.*, 2021, 60: 21751–21755.

[98] Yang, P. Z.; Cao, Z. H.; Long, Y. H.; Liu, D. F.; Huang, W. L.; Zhan, S. H.; Li, M. Regulating the local electronic structure of copper single atoms with unsaturated B, O-coordination for selective $^1O_2$ generation. *ACS Catal.*, 2023, 13(18): 12414–12424.

[99] Song, J. S.; Hou, N. N.; Liu, X. C.; Antonietti, M.; Zhang, P. J.; Ding, R. R.; Song, L.; Wang, Y.; Mu, Y. Asymmetrically coordinated CoB1N3 moieties for selective generation of high-valence co-oxo species *via* coupled electron–proton transfer in Fenton-like reactions. *Adv. Mater.*, 2023, 35: 2209552.

[100] Mi, X. Y.; Wang, P. F.; Xu, S. Z.; Su, L. N.; Zhong, H.; Wang, H. T.; Li, Y.; Zhan, S. H. Almost 100 % peroxymonosulfate conversion to singlet oxygen on single-atom $CoN^{2+}2$ sites. *Angew. Chem. Int. Ed.*, 2021, 60: 4588–4593.

[101] Han, B.; Luo, Y.; Lin, Y. F.; Weng, B.; Xia, D. H.; Zhou, Y.; Guan, C. T.; Wang, Z.; Wei, X. P.; Jiang, J. Microenvironment engineering of single-atom catalysts for persulfate-based advanced oxidation processes. *Chem. Eng. J.*, 2022, 447: 137551.

[102] Li, J. M.; Yang, Z. X.; Li, Y.; Zhang, G. K. Advances in single-atom catalysts: Design, synthesis and environmental applications. *J. Hazard. Mater.*, 2022, 429: 128285.

[103] Zhang, J. J.; Tang, X.; Hong, Y. J.; Chen, G. Y.; Chen, Y.; Zhang, L.; Gao, W. R.; Zhou, Y.; Sun, B. Carbon-based single-atom catalysts in advanced oxidation reactions for water remediation: From materials to reaction pathways. *Eco Environ. Health*, 2023, 2: 47–60.

[104] Wang, S. B.; Hou, X. L.; Li, Y. C.; Zhou, C.; Zhang, P.; Hu, C. From single-atom to dual-atom: A universal principle for the rational design of heterogeneous Fenton-like catalysts. *Environ. Sci. Technol.*, 2025, 59(17): 8822–8833.

[105] Gao, Y.; Wu, T. W.; Yang, C. D.; Ma, C.; Zhao, Z. Y.; Wu, Z. H.; Cao, S. J.; Geng, W.; Wang, Y.; Yao, Y. Y. et al. Activity trends and mechanisms in peroxymonosulfate-assisted catalytic production of singlet oxygen over atomic metal-N-C catalysts. *Angew. Chem. Int. Ed.*, 2021, 60: 22513–22521.

[106] Miao, J.; Zhu, Y.; Lang, J. Y.; Zhang, J. Z.; Cheng, S. X.; Zhou, B. X.; Zhang, L. Z.; Alvarez, P. J. J.; Long, M. C. Spin-state-dependent peroxymonosulfate activation of single-atom M–N moieties *via* a radical-free pathway. *ACS Catal.*, 2021, 11: 9569–9577.

[107] Liang, X. Y.; Wang, D.; Zhao, Z. Y.; Li, T.; Gao, Y. W.; Hu, C. Coordination number dependent catalytic activity of single-atom cobalt catalysts for Fenton-like reaction. *Adv. Funct. Mater.*, 2022, 32: 2203001.

[108] Yin, K. X.; Wu, R. X.; Shang, Y. N.; Chen, D. D.; Wu, Z. L.; Wang, X. H.; Gao, B. Y.; Xu, X. Microenvironment modulation of cobalt single-atom catalysts for boosting both radical oxidation and electron-transfer process in Fenton-like system. *Appl. Catal. B Environ.*, 2023, 329: 122558.

[109] Jin, S. J.; Tan, W. X.; Tang, X. F.; Li, M. X.; Yu, X. Y.; Zhang, H. Y.; Song, S.; Zeng, T. Unraveling the fundamentals of axial coordination $FeN^{4+}1$ sites regulating the peroxymonosulfate activation for Fenton-like activity. *Small*, 2024, 20: 2405012.

[110] Zhang, H. C.; Cui, P. X.; Xie, D. H.; Wang, Y. J.; Wang, P.; Sheng, G. P. Axial N ligand-modulated ultrahigh activity and selectivity hyperoxide activation over single-atoms nanozymes. *Adv. Sci.*, 2023, 10: 2205681.

[111] Du, Q.; Zhu, C. Q.; Yue, C. L.; Cun, F. X.; Du, Z. L.; Liu, F. Q.; Li, A. M. Anchoring atomically dispersed FeN_5 sites on porous and defect-rich biochar *via* cascade regulation strategy for efficient Fenton-like catalysis. *Appl. Catal. B Environ.*, 2024, 343: 123570.

[112] Ma, T. G.; Liu, M. J.; Li, T. T.; Ren, H. J.; Zhou, R. Nitrogen-doped carbon nanotubes derived from carbonized polyaniline as a robust peroxydisulfate activator for the oxidation removal of organic pollutants: Singlet oxygen dominated mechanism and structure-activity relationship. *Sep. Purif. Technol.*, 2022, 293: 121124.

[113] Chang, L.; Xue, X. J.; Deng, Q. C.; Xie, X. Y.; Zhang, X. D.; Cheng, C.; Chai, H. X.; Huang, Y. M. Modulating the electronic structure of Co center *via* MgO@C co-doping for PMS activation to remove levofloxacin. *Sep. Purif. Technol.*, 2023, 321: 124151.

[114] Jiang, Z. Y.; Shi, Z. L.; Li, C.; Wang, H. Q.; Huang, Y. P.; Ye, L. Q. Nitrogen-doped carbon materials for persulfate activation *via* electron transfer pathways. *Langmuir*, 2024, 40(39): 20584–20595.

[115] Shang, H. S.; Zhou, X. Y.; Dong, J. C.; Li, A.; Zhao, X.; Liu, Q. H.; Lin, Y.; Pei, J. J.; Li, Z.; Jiang, Z. L. et al. Engineering unsymmetrically coordinated Cu-S(1)N(3) single atom sites with enhanced oxygen reduction activity. *Nat. Commun.*, 2020, 11: 3049.

[116] Gao, Y. W.; Zhu, Y.; Li, T.; Chen, Z. H.; Jiang, Q. K.; Zhao, Z. Y.; Liang, X. Y.; Hu, C. Unraveling the high-activity origin of single-atom iron catalysts for organic pollutant oxidation *via* peroxymonosulfate activation. *Environ. Sci. Technol.*, 2021, 55(12): 8318–8328.

[117] Zhao, X.; Gong, Z. H.; Cai, B. X.; Li, X. T.; Liao, Y.; Gou, S. Y.; Chen, K. D.; Song, L. J.; Wang, Q.; Ma, J. Significantly improved H_2O_2 utilization efficiency over $CuFeO_2$ Fenton-like catalyst through elevating Lewis acidity. *Mater. Sci. Semicond. Process.*, 2024, 179: 108531.

[118] Pei, Y.; Liu, X.; Cao, M. B.; Wang, Z. J.; Yang, H. B. Heteroatom-modulated $NiCo_2O_4$ apparent energy activation of PMS for tetracycline removal: Mechanism and toxicity analysis. *Environ. Res.*, 2024, 240: 117571.

[119] Feng, X. C.; Xiao, Z. J.; Shi, H. T.; Zhou, B. Q.; Wang, Y. M.; Chi, H. Z.; Kou, X. H.; Ren, N. Q. How nitrogen and sulfur doping modified material structure, transformed oxidation pathways, and improved degradation performance in peroxymonosulfate activation. *Environ. Sci. Technol.*, 2022, 56(19): 14048–14058.

[120] Hu, J. H.; Li, Y.; Zou, Y. B.; Lin, L.; Li, B.; Li, X. Y. Transition metal single-atom embedded on N-doped carbon as a catalyst for peroxymonosulfate activation: A DFT study. *Chem. Eng. J.*, 2022, 437: 135428.

[121] Long, Y. H.; Cao, Z. H.; Wu, W. R.; Liu, W. H.; Yang, P. Z.; Zhan, X. S.; Chen, R. Z.; Liu, D. F.; Huang, W. L. Rational modulation of Fe single-atom electronic structure in a Fe-N_2B_4 configuration for preferential $^1O_2$ generation in Fenton-like reactions. *Appl. Catal. B Environ. Energy*, 2024, 344: 123643.

[122] Shen, Y.; Yang, M. Z.; Zhu, C.; Zhang, H. Z.; Liu, R. L.; Wang, J.; Fang, Q. L.; Song, S.; Chen, B. L. Enhanced selectivity in PMS activation *via* non-metal doping for efficient $^1O_2$ generation in emerging organic pollutants degradation. *ACS ES&T Engg.*, 2024, 4(11): 2839–2851.

[123] Sun, W. X.; Liu, G. S.; Zou, H.; Wang, S. B.; Duan, X. G. Site-designed dual-active-center catalysts for co-catalysis in advanced oxidation processes. *NPJ Mater. Sustain.*, 2025, 3: 2.

[124] Zhou, Q. X.; Song, C. L.; Wang, P. F.; Zhao, Z. Y.; Li, Y.; Zhan, S. H. Generating dual-active species by triple-atom sites through peroxymonosulfate activation for treating micropollutants in complex water. *Proc. Natl. Acad. Sci. USA*, 2023, 120: e2300085120.

[125] Xie, Z. Q.; Dionysiou, D. D.; Luo, S.; Chen, M. L.; Wei, Z. S. Dual-reaction center catalyst based on common metals Cu-Mg-Al for synergistic peroxymonosulfate adsorption-activation in Fenton-like process. *Appl. Catal. B Environ.*, 2023, 327: 122468.

[126] Wang, Z. J.; Bao, J. G.; He, H. Z.; Mukherji, S.; Luo, L. T.; Du, J. K. Single-Atom iron catalyst activating peroxydisulfate for efficient organic contaminant degradation relying on electron transfer. *Chem. Eng. J.*, 2023, 458: 141513.

[127] Chen, Q. M.; Liu, Y.; Lu, Y. W.; Hou, Y. J.; Zhang, X. D.; Shi, W. B.; Huang, Y. M. Atomically dispersed Fe/Bi dual active sites single-atom nanozymes for cascade catalysis and peroxymonosulfate

activation to degrade dyes. *J. Hazard. Mater.*, 2022, 422: 126929.
[128] Wang, F.; Gao, Y.; Fu, H. F.; Liu, S. S.; Wei, Y. W.; Wang, P.; Zhao, C.; Wang, J. F.; Wang, C. C. Almost 100 % electron transfer regime over Fe–Co dual-atom catalyst toward pollutants removal: Regulation of peroxymonosulfate adsorption mode. *Appl. Catal. B Environ.*, 2023, 339: 123178.
[129] Xie, Z. Q.; Lyu, Z. P.; Wang, J. N.; Li, A. M.; François-Xavier Corvini, P. Ultrafine-Mn_2O_3@N-doped porous carbon hybrids derived from Mn-MOFs: Dual-reaction centre catalyst with singlet oxygen-dominant oxidation process. *Chem. Eng. J.*, 2022, 429: 132299.
[130] Sun, Y. T.; Hu, C.; Lyu, L. New sustainable utilization approach of livestock manure: Conversion to dual-reaction-center Fenton-like catalyst for water purification. *NPJ Clean Water*, 2022, 5: 53.
[131] Lyu, L.; Lu, C.; Sun, Y. T.; Cao, W. R.; Gao, T. T.; Hu, C. Low consumption Fenton-like water purification through pollutants as electron donors substituting H_2O_2 consumption *via* twofold cation-π over MoS_2 cross-linking g-C_3N_4 hybrid. *Appl. Catal. B Environ.*, 2023, 320: 121871.
[132] Lu, C.; Hu, C.; Rong, H. W.; Lyu, L. Low-consumption water purification: Trace H_2O_2 triggering H_2O_2 generation through pollutant utilization on non-equilibrium ZnS surface. *Appl. Catal. B Environ.*, 2023, 338: 123051.
[133] Liu, J. M.; Cao, W. R.; Liu, S. Q.; Sun, Y. T.; Mao, L. S.; Chen, X.; Fang, Y. F.; Hu, C.; Lyu, L. H_2O_2 generation for water purification induced by trace peroxymonosulfate on surface of Ca-C biochar converted from pigeon manure. *J. Environ. Chem. Eng.*, 2025, 13: 115061.
[134] Sun, Y. T.; Hu, C.; Lyu, L. H_2O_2 triggering electron-directed transfer of emerging contaminants over asymmetric nano zinc oxide surfaces for water self-purification expansion. *JACS Au*, 2025, *5*(1), 271–280.
[135] Lu, C.; Hu, C.; Wu, J. M.; Rong, H. W.; Lyu, L. Endogenous substances utilization for water self-purification amplification driven by nonexpendable H_2O_2 over a micro-potential difference surface. *Environ. Sci. Technol.*, 2024, 58(52): 23241–23250.
[136] Wang, Z. W.; Almatrafi, E.; Wang, H.; Qin, H.; Wang, W. J.; Du, L.; Chen, S.; Zeng, G. M.; Xu, P. Cobalt single atoms anchored on oxygen-doped tubular carbon nitride for efficient peroxymonosulfate activation: Simultaneous coordination structure and morphology modulation. *Angew. Chem. Int. Ed.*, 2022, 61: e202202338.
[137] Li, J. S.; Wang, Y. S.; Wang, Z. Q.; Ding, D. H. Triggering nanoconfinement effect in advanced oxidation processes (AOPs) for boosted degradation of organic contaminants: A review. *Chem. Eng. J.*, 2025, 503: 158428.
[138] Dai, H. X.; Li, N.; Ye, J. Y.; Zhao, J. H.; He, X.; Duan, X. G.; Yan, B. B.; Chen, G. Y.; Wang, S. B. Confinement boosted heterogeneous advanced oxidation processes. *Chem. Eng. J.*, 2023, 472: 144861.
[139] Li, Y. W.; Zhao, M. B.; Ma, W. L.; Ma, T. Y.; Wang, S. B.; Duan, X. G. Nanoconfinement in ordered mesopores materials for catalytic wastewater purification. *Chem. Eng. J.*, 2025, 504: 156407.
[140] Yang, D. D.; Xie, C.; Li, Y. L.; Wu, Z. J.; Li, Y. H.; Lu, J. D.; Hong, P. D.; He, J. Y.; Zhu, Z. G.; Kong, L. T. Enhanced tetracycline degradation through nonradical processes by modulating the exposure of active sites on the iron nanoconfined catalysts. *Sep. Purif. Technol.*, 2024, 349: 127878.
[141] Liu, Y.; Wang, Y. Y.; Li, X.; Zhang, X. F.; Fang, M.; Zheng, L. Y.; Li, Y. W.; Ren, J. Y.; Guo, H.; Ma, Q. L. et al. Multi-path accelerating sulfadiazine degradation *via* peracetic acid oxidation induced by nanoconfined co species: Highlighting electron rearrangement effect. *Chem. Eng. J.*, 2024, 494: 153167.
[142] Qian, J. S.; Gao, X.; Pan, B. C. Nanoconfinement-mediated water treatment: From fundamental to application. *Environ. Sci. Technol.*, 2020, 54(14): 8509–8526.
[143] Huang, B. K.; Wu, Z. L.; Wang, X. H.; Song, X. Y.; Zhou, H. Y.; Zhang, H.; Zhou, P.; Liu, W.; Xiong, Z. K.; Lai, B. Coupled surface-confinement effect and pore engineering in a single-Fe-atom catalyst for ultrafast Fenton-like reaction with high-valent iron-oxo complex oxidation. *Environ. Sci. Technol.*, 2023, 57(41): 15667–15679.
[144] Wu, W. J.; Guo, J.; Wang, W. H.; Yu, X. M.; Wang, Y. F.; Zhou, T.; Yin, G. S. Nanoconfined catalytic membranes for EfOM fouling mitigation: An intelligent "pore-centric" cleaning strategy. *J. Membr. Sci.*, 2025, 715: 123444.
[145] Zhou, C. D.; Guo, Y. L.; Du, S. H.; Sui, M. H. Ultrafast Fenton-like reaction using a peroxymonosulfate-mediated confined-Fe^0 catalyst for the degradation of sulfamethoxazole. *Appl. Catal. B Environ. Energy*, 2024, 358: 124442.
[146] Liu, T. C.; Xiao, S. Z.; Li, N.; Chen, J. B.; Zhou, X. F.; Qian, Y. J.; Huang, C. H.; Zhang, Y. L. Water decontamination *via* nonradical process by nanoconfined Fenton-like catalysts. *Nat. Commun.*, 2023, 14: 2881.
[147] Cui, J. H.; Shao, S. T.; Li, L. N.; Zhang, P.; Cui, J. G.; Hu, C.; Zhao, Y. B. Nanoconfinement-regulated peroxymonosulfate activation *via* an anomalously efficient mediated electron-transfer pathway on cobalt. *ACS ES&T Engg.*, 2022, 2(11): 2014–2022.
[148] Meng, Y.; Liu, Y. Q.; Wang, C.; Si, Y.; Wang, Y. J.; Xia, W. Q.; Liu, T.; Cao, X.; Guo, Z. Y.; Chen, J. J. et al. Nanoconfinement steers non-radical pathway transition in single atom Fenton-like catalysis for improving oxidant utilization. *Nat. Commun.*, 2024, 15: 5314.
[149] Xiang, M. H.; Zhu, S. T.; Ren, X. L.; Yang, Z. Y.; Wang, C.; Chen, L.; Zhang, J.; Li, H. Fast diffusion kinetics improves electron transfer regime selectivity to boost peroxymonosulfate activation. *Chem. Eng. J.*, 2024, 497: 154983.
[150] Feng, C.; Zhang, H.; Liu, Y.; Ren, Y.; Zhou, P.; He, C. S.; Xiong, Z. K.; Liu, W. H.; Dai, X. Q.; Lai, B. Surface structure regulation of sulfidated zero-valent iron by H_2O_2 for efficient pH self-regulation and proton cycle to boost heterogeneous Fenton-like reaction for pollutant control. *Appl. Catal. B Environ. Energy*, 2024, 345: 123667.
[151] Mei, S. C.; Li, L.; Huang, G. X.; Pan, X. Q.; Yu, H. Q. Heterogeneous Fenton water purification catalyzed by iron phosphide (FeP). *Water Res.*, 2023, 241: 120151.
[152] Yan, Q. Y.; Lian, C.; Huang, K.; Liang, L. H.; Yu, H. R.; Yin, P. C.; Zhang, J. L.; Xing, M. Y. Constructing an acidic microenvironment by MoS_2 in heterogeneous Fenton reaction for pollutant control. *Angew. Chem. Int. Ed.*, 2021, 60: 17155–17163.
[153] Meng, X.; Zhang, F.; Guo, H. L.; Zhang, C. Y.; Hu, H. T.; Wang, W.; Liu, J.; Shuai, X. T.; Cao, Z. One-pot approach to Fe^{2+}/Fe^{3+}-based MOFs with enhanced catalytic activity for Fenton reaction. *Adv. Healthc. Mater.*, 2021, 10: 2100780.
[154] Wu, J. Y.; Lin, H.; Moss, D. J.; Loh, K. P.; Jia, B. H. Graphene oxide for photonics, electronics and optoelectronics. *Nat. Rev. Chem.*, 2023, 7: 162–183.
[155] Xu, S. L.; Wang, W.; Song, Y.; Tang, R.; Hu, Z. H.; Zhou, X.; Yu, H. Q. Expanding the pH range of Fenton-like reactions for pollutant degradation: The impact of acidic microenvironments. *Water Res.*, 2025, 270: 122851.
[156] Cui, L. L.; Zhao, X. Y.; Xie, H. J.; Zhang, Z. H. Overcoming the activity–stability trade-off in heterogeneous electro-Fenton catalysis: Encapsulating carbon cloth-supported iron oxychloride within graphitic layers. *ACS Catal.*, 2022, 12(21): 13334–13348.
[157] Zhang, L.; Qi, J. J.; Fang, Z. M.; Xing, L.; Li, Q. W.; Li, X. Z.; Liu, S.; Wang, X. K.; Wang, L. D. Interlayer-confined strategy to modulate alkaline reaction microenvironment for *in-situ* degradation of ofloxacin. *Appl. Catal. B Environ. Energy*, 2024, 357: 124339.
[158] Bokare, A. D.; Choi, W. Review of iron-free Fenton-like systems for activating H_2O_2 in advanced oxidation processes. *J. Hazard.*

Mater., 2014, 275: 121–135.
[159] Yang, T. Y.; Yu, D. Y.; Wang, D.; Yang, T.; Li, Z. X.; Wu, M. H.; Petru, M.; Crittenden, J. Accelerating Fe(III)/Fe(II) cycle *via* Fe(II) substitution for enhancing Fenton-like performance of Fe-MOFs. *Appl. Catal. B Environ.*, 2021, 286: 119859.
[160] Toda, K.; Tanaka, T.; Tsuda, Y.; Ban, M.; Koveke, E. P.; Koinuma, M.; Ohira, S. I. Sulfurized limonite as material for fast decomposition of organic compounds by heterogeneous Fenton reaction. *J. Hazard. Mater.*, 2014, 278: 426–432.
[161] Chen, Z.; Li, J.; Yang, B.; Cao, J. Z.; Zhu, L. L.; Xing, M. Y. Regulating lewis acid-base sites over Fenton system for enhancing degradation of pollutants in saline and buffered wastewater. *Chin. J. Chem.*, 2024, 42: 2563–2571.
[162] Tian, H. R.; Cui, K. P.; Sun, S. J.; Li, H. Y.; Chen, X. Construction of acidic microenvironments to overcome the pH dependence of iron-based catalysts and application to the degradation of micropollutants by AOPs. *Chem. Eng. J.*, 2024, 488: 150934.
[163] Chang, K.; Mei, Z. W.; Wang, T.; Kang, Q.; Ouyang, S. X.; Ye, J. H. MoS_2/graphene cocatalyst for efficient photocatalytic H_2 evolution under visible light irradiation. *ACS Nano*, 2014, 8(7): 7078–7087.
[164] Zhou, H. Y.; Lai, L. D.; Wan, Y. J.; He, Y. L.; Yao, G.; Lai, B. Molybdenum disulfide (MoS_2): A versatile activator of both peroxymonosulfate and persulfate for the degradation of carbamazepine. *Chem. Eng. J.*, 2020, 384: 123264.
[165] Tian, Q. B.; Chang, J. L.; Yu, B. L.; Jiang, Y.; Gao, B. Y.; Yang, J. R.; Li, Q.; Gao, Y.; Xu, X. Co-catalysis strategy for low-oxidant-consumption Fenton-like chemistry: From theoretical understandings to practical applications and future guiding strategies. *Water Res.*, 2024, 267: 122488.
[166] Liang, Z. Y.; Yan, Q. Y.; Ou, H. S.; Li, D. W.; Zhang, Y. Y.; Zhang, J. L.; Zeng, L. X.; Xing, M. Y. Effective green treatment of sewage sludge from Fenton reactions: Utilizing MoS_2 for sustainable resource recovery. *Proc. Natl. Acad. Sci. USA*, 2024, 121: e2317394121.
[167] Zhang, X. K.; Liu, J.; Zhang, H. Z.; Wan, Z.; Li, J. Uncovering the pathway of peroxymonosulfate activation over $Co_{0.5}Zn_{0.5}O$ nanosheets for singlet oxygen generation: Performance and membrane application. *Appl. Catal. B Environ.*, 2023, 327: 122429.
[168] Yang, Z. Y.; Li, X.; Huang, Y. Z.; Chen, Y. W.; Wang, A. Q.; Wang, Y. C.; Li, C. H.; Hu, Z. F.; Yan, K. Facile synthesis of cobalt-iron layered double hydroxides nanosheets for direct activation of peroxymonosulfate (PMS) during degradation of fluoroquinolones antibiotics. *J. Clean. Prod.*, 2021, 310: 127584.
[169] Wang, Q.; Xu, Z. T.; Cao, Y. T.; Chen, Y. Q.; Du, X.; Yang, Y.; Wang, Z. H. Two-dimensional ultrathin perforated Co_3O_4 nanosheets enhanced PMS-Activated selective oxidation of organic micropollutants in environmental remediation. *Chem. Eng. J.*, 2022, 427: 131953.
[170] Wei, Y.; Miao, J.; Ge, J. X.; Lang, J. Y.; Yu, C. Y.; Zhang, L. Z.; Alvarez, P. J. J.; Long, M. C. Ultrahigh peroxymonosulfate utilization efficiency over CuO nanosheets *via* heterogeneous Cu(III) formation and preferential electron transfer during degradation of phenols. *Environ. Sci. Technol.*, 2022, 56(12): 8984–8992.
[171] Guo, X.; Zhang, H.; Yao, Y. Y.; Xiao, C. M.; Yan, X.; Chen, K.; Qi, J. W.; Zhou, Y. J.; Zhu, Z. G.; Sun, X. Y. et al. Derivatives of two-dimensional MXene-MOFs heterostructure for boosting peroxymonosulfate activation: Enhanced performance and synergistic mechanism. *Appl. Catal. B Environ.*, 2023, 323: 122136.
[172] Cao, M. B.; Zhang, H. M.; Wei, X. Y. Enhanced Fenton-like rate and anti-interference through designing materials with specific excellent sorption to pollutant. *Chem. Eng. J.*, 2024, 502: 158046.
[173] Solís, R. R.; Mena, I. F.; Nadagouda, M. N.; Dionysiou, D. D. Adsorptive interaction of peroxymonosulfate with graphene and catalytic assessment *via* non-radical pathway for the removal of aqueous pharmaceuticals. *J. Hazard. Mater.*, 2020, 384: 121340.
[174] Fu, Q.; Yang, H. S.; Yu, J. X.; Li, N.; Tong, Y. J.; Wei, S. B.; Hao, Z. P.; Wang, J. H.; Ouyang, G. F. Porous carbon nano-sheets as excellent carbocatalysts for organic pollutant removal *via* persulfate activation: The role of the sp^2/sp^3 carbon ratio. *Environ. Sci.: Nano*, 2022, 9: 1748–1758.
[175] Chu, C. H.; Yang, J.; Huang, D. H.; Li, J. F.; Wang, A. Q.; Alvarez, P. J. J.; Kim, J. H. Cooperative pollutant adsorption and persulfate-driven oxidation on hierarchically ordered porous carbon. *Environ. Sci. Technol.*, 2019, 53(17): 10352–10360.
[176] Qiu, X. J.; Zhao, Y. X.; Li, C. X.; Song, Y. X.; Mutabazi, E.; Yang, S. J.; Sun, P. Z.; Wang, S. B. Micropores-confined peroxymonosulfate activation for enhanced catalytic performance and durability. *Chem. Eng. J.*, 2024, 483: 149265.
[177] Li, K. L.; Zhang, Y.; Xu, L. L.; Liu, L.; Wang, Z. Y.; Hou, D. Y.; Wang, Y. J.; Wang, J. Mass transfer and interfacial reaction mechanisms in a novel electro-catalytic membrane contactor for wastewater treatment by O_3. *Appl. Catal. B Environ.*, 2020, 264: 118512.
[178] Wei, K. J.; Wang, Z.; Ouyang, C. P.; Cao, X. X.; Liang, P.; Huang, X.; Zhang, X. Y. A hybrid fluidized-bed reactor (HFBR) based on arrayed ceramic membranes (ACMs) coupled with powdered activated carbon (PAC) for efficient catalytic ozonation: A comprehensive study on a pilot scale. *Water Res.*, 2020, 173: 115536.
[179] Lee, W. J.; Bao, Y. P.; Hu, X.; Lim, T. T. Hybrid catalytic ozonation-membrane filtration process with CeO_x and MnO_x impregnated catalytic ceramic membranes for micropollutants degradation. *Chem. Eng. J.*, 2019, 378: 121670.
[180] Xiao, C.; Hu, Y. Y.; Li, Q. T.; Liu, J. Y.; Li, X.; Shi, Y. Y.; Chen, Y. C.; Cheng, J. H.; Zhu, X. Q.; Wang, G. B. et al. Degradation of sulfamethoxazole by super-hydrophilic MoS_2 sponge co-catalytic Fenton: Enhancing Fe^{2+}/Fe^{3+} cycle and mass transfer. *J. Hazard. Mater.*, 2023, 458: 131878.
[181] Lu, H. Y.; Hou, L. F.; Zhang, Y.; Cao, X. Q.; Xu, X.; Shang, Y. N. Pilot-scale and large-scale Fenton-like applications with nano-metal catalysts: From catalytic modules to scale-up applications. *Water Res.*, 2024, 266: 122425.
[182] Ly, Q. V.; Cui, L. L.; Asif, M. B.; Khan, W.; Nghiem, L. D.; Hwang, Y.; Zhang, Z. H. Membrane-based nanoconfined heterogeneous catalysis for water purification: A critical review ☆. *Water Res.*, 2023, 230: 119577.
[183] Wang, Z.; Meng, C. C.; Zhang, W.; Zhang, S. Z.; Yang, B.; Zhang, Z. H. Honeycomb-like holey Co_3O_4 membrane triggered peroxymonosulfate activation for rapid degradation of organic contaminants. *Sci. Total Environ.*, 2022, 814: 152698.
[184] Zhang, J.; Ma, Y. L.; Sun, Y. G.; Wang, L.; Wang, L. Q.; Wang, Z.; Zhao, B. L.; Gao, J. D.; Xu, M. Ultrahigh-flux 2D CoO@MoS_2 composite membrane activated peroxymonosulfate through enhanced electron transfer for rapid degradation of refractory benzotriazole. *Chem. Eng. J.*, 2023, 471: 144837.
[185] Joshi, R. K.; Carbone, P.; Wang, F. C.; Kravets, V. G.; Su, Y.; Grigorieva, I. V.; Wu, H. A.; Geim, A. K.; Nair, R. R. Precise and ultrafast molecular sieving through graphene oxide membranes. *Science*, 2014, 343: 752–754.
[186] Meng, C. C.; Wang, Z.; Zhang, W.; Cui, L. L.; Yang, B.; Xie, H. J.; Zhang, Z. H. Laminar membranes assembled by ultrathin cobalt-copper oxide nanosheets for nanoconfined catalytic degradation of contaminants. *Chem. Eng. J.*, 2022, 449: 137811.
[187] Xu, P.; Wei, R.; Wang, P.; Shen, T. Y.; Zheng, T.; Zhang, G. S. A nanoconfined $FeCo_2O_4$-embedded ceramic membrane regulates electron transfer in peroxymonosulfate activation to selectively generate singlet oxygen for water decontamination. *Environ. Sci. Technol.*, 2024, 58(39): 17464–17474.
[188] Asif, M. B.; Iftekhar, S.; Maqbool, T.; Pramanik, B. K.; Tabraiz, S.;

Sillanpää, M.; Zhang, Z. H. Two-dimensional nanoporous and lamellar membranes for water purification: Reality or a myth. *Chem. Eng. J.*, 2022, 432: 134335.

[189] Meng, C. C.; Ding, B. F.; Zhang, S. Z.; Cui, L. L.; Ostrikov, K. K.; Huang, Z. Y.; Yang, B.; Kim, J. H.; Zhang, Z. H. Angstrom-confined catalytic water purification within Co-TiOx laminar membrane nanochannels. *Nat. Commun.*, 2022, 13: 4010.

[190] Ni, L. F.; Wang, P. F.; Westerhoff, P.; Luo, J. Y.; Wang, K. C.; Wang, Y. Y. Mechanisms and strategies of advanced oxidation processes for membrane fouling control in MBRs: Membrane-foulant removal versus mixed-liquor improvement. *Environ. Sci. Technol.*, 2024, 58(26): 11213–11235.

[191] Zhang, G. C.; Yang, X. Y.; Wu, Z. X.; Wu, W. D.; Wang, X. N.; Chen, X. D.; Sun, S. P. Fe-Mn bimetallic oxide-enabled facile cleaning of microfiltration ceramic membranes for effluent organic matter fouling mitigation *via* activation of oxone. *ACS EST Water*, 2022, 2(7): 1234–1246.

[192] Wang, Y. J.; Li, C. X.; Meng, Y.; Guo, Z. Y.; Cui, S.; Fu, X. Z.; Liu, H. Q.; Xia, W. Q.; Li, W. W. Coagulation/co-catalytic membrane integrated system for fouling-resistant and efficient water purification. *Water Res.*, 2024, 250: 121055.

[193] You, Y.; Jin, X. H.; Wen, X. Y.; Sahajwalla, V.; Chen, V.; Bustamante, H.; Joshi, R. K. Application of graphene oxide membranes for removal of natural organic matter from water. *Carbon*, 2018, 129: 415–419.

[194] Zhang, S.; Hedtke, T.; Zhu, Q. H.; Sun, M.; Weon, S.; Zhao, Y. M.; Stavitski, E.; Elimelech, M.; Kim, J. H. Membrane-confined iron oxychloride nanocatalysts for highly efficient heterogeneous Fenton water treatment. *Environ. Sci. Technol.*, 2021, 55(13): 9266–9275.

[195] Lin, T. X.; Wen, X. Y.; Ren, X. J.; Quintano, V.; Andreeva, D. V.; Novoselov, K. S.; Joshi, R. Recent advances in graphene-based membranes with nanochannels and nanopores. *Small Struct.*, 2025, 6: 2400320.

[196] Tian, M. T.; Liu, Y.; Zhang, S. Z.; Yu, C.; Ostrikov, K. K.; Zhang, Z. H. Overcoming the permeability-selectivity challenge in water purification using two-dimensional cobalt-functionalized vermiculite membrane. *Nat. Commun.*, 2024, 15: 391.

[197] Cai, Q. Q.; Wu, M. Y.; Hu, L. M.; Lee, B. C. Y.; Ong, S. L.; Wang, P.; Hu, J. Y. Organics removal and *in situ* granule activated carbon regeneration in FBR-Fenton/GAC process for reverse osmosis concentrate treatment. *Water Res.*, 2020, 183: 116119.

[198] Zhuang, C. J.; Yan, Y. Sulfur and nitrogen Co-doped carbon nanotube membrane coating on paper-like sintered stainless steel fibres for catalytic phenol degradation in structured fixed-bed reactor. *Sep. Purif. Technol.*, 2025, 354: 129557.

[199] Esteves, B. M.; Morales-Torres, S.; Maldonado-Hódar, F. J.; Madeira, L. M. Sustainable iron-olive stone-based catalysts for Fenton-like olive mill wastewater treatment: Development and performance assessment in continuous fixed-bed reactor operation. *Chem. Eng. J.*, 2022, 435: 134809.

[200] Cai, Q. Q.; Lee, B. C. Y.; Ong, S. L.; Hu, J. Y. Fluidized-bed Fenton technologies for recalcitrant industrial wastewater treatment–Recent advances, challenges and perspective. *Water Res.*, 2021, 190: 116692.

[201] Zhang, X. W.; Lan, M. Y.; Wang, F.; Wang, C. C.; Wang, P.; Ge, C. J.; Liu, W. Immobilized N-C/Co derived from ZIF-67 as PS-AOP catalyst for effective tetracycline matrix elimination: From batch to continuous process. *Chem. Eng. J.*, 2022, 450: 138082.

[202] Huang, M. J.; Li, Y. S.; Zhang, C. Q.; Cui, C.; Huang, Q. Q.; Li, M. K.; Qiang, Z. M.; Zhou, T.; Wu, X. H.; Yu, H. Q. Facilely tuning the intrinsic catalytic sites of the spinel oxide for peroxymonosulfate activation: From fundamental investigation to pilot-scale demonstration. *Proc. Natl. Acad. Sci. USA*, 2022, 119: e2202682119.

[203] Ziembowicz, S.; Kida, M. Limitations and future directions of application of the Fenton-like process in micropollutants degradation in water and wastewater treatment: A critical review. *Chemosphere*, 2022, 296: 134041.

[204] Tisa, F.; Abdul Raman, A. A.; Wan Daud, W. M. A. Applicability of fluidized bed reactor in recalcitrant compound degradation through advanced oxidation processes: A review. *J. Environ. Manag.*, 2014, 146: 260–275.

[205] Li, B. R.; Guo, Z. W.; Cui, Y. H.; Feng, Y. H.; Wu, C. D.; Meng, M. J. LDHs-based 3D modular foam with double metal-fluorine interaction for efficiently promoting peroxymonosulfate activation in water pollutant control. *Chem. Eng. J.*, 2021, 425: 131541.

[206] Hu, X. N.; Zhu, M. S. Were persulfate-based advanced oxidation processes really understood? basic concepts, cognitive biases, and experimental details. *Environ. Sci. Technol.*, 2024, 58: 10415–10444.

[207] Zhang, P.; Sun, M. L.; Zhou, C. Y.; He, C. S.; Liu, Y.; Zhang, H.; Xiong, Z. K.; Liu, W.; Zhou, P.; Lai, B. Origins of selective oxidation in carbon-based nonradical oxidation processes toward organic pollutants: Quantitative structure–activity relationships (QSARs). *Environ. Sci. Technol.*, 2024, 58(10): 4781–4791.

[208] Ding, Y. B.; Wang, X. R.; Fu, L. B.; Peng, X. Q.; Pan, C.; Mao, Q. H.; Wang, C. J.; Yan, J. C. Nonradicals induced degradation of organic pollutants by peroxydisulfate (PDS) and peroxymonosulfate (PMS): Recent advances and perspective. *Sci. Total Environ.*, 2021, 765: 142794.

[209] Yan, Y. Q.; Wei, Z. S.; Duan, X. G.; Long, M. C.; Spinney, R.; Dionysiou, D. D.; Xiao, R. Y.; Alvarez, P. J. J. Merits and limitations of radical *vs.* nonradical pathways in persulfate-based advanced oxidation processes. *Environ. Sci. Technol.*, 2023, 57(33): 12153–12179.

[210] Luo, S.; Wei, Z. S.; Spinney, R.; Villamena, F. A.; Dionysiou, D. D.; Chen, D.; Tang, C. J.; Chai, L. Y.; Xiao, R. Y. Quantitative structure–activity relationships for reactivities of sulfate and hydroxyl radicals with aromatic contaminants through single–electron transfer pathway. *J. Hazard. Mater.*, 2018, 344: 1165–1173.

[211] Hansch, C.; Leo, A.; Taft, R. W. A survey of Hammett substituent constants and resonance and field parameters. *Chem. Rev.*, 1991, 91(2): 165–195.

[212] Guan, C. T.; Jiang, J.; Pang, S. Y.; Luo, C. W.; Ma, J.; Zhou, Y.; Yang, Y. Oxidation kinetics of bromophenols by nonradical activation of peroxydisulfate in the presence of carbon nanotube and formation of brominated polymeric products. *Environ. Sci. Technol.*, 2017, 51(18): 10718–10728.

[213] Liu, J. Q.; Wu, P. X.; Yang, S. S.; Rehman, S.; Ahmed, Z.; Zhu, N. W.; Dang, Z.; Liu, Z. H. A photo-switch for peroxydisulfate non-radical/radical activation over layered CuFe oxide: Rational degradation pathway choice for pollutants. *Appl. Catal. B Environ.*, 2020, 261: 118232.

[214] Liu, X. Y.; Cui, K. P.; Yao, Y. L.; Chen, X.; Li, C. X.; Chen, Y. H.; Hu, Z. H.; Cui, M. S. Enhanced removal of phenolic pollutants over MnO_2 initiated by peracetic acid: *in situ* generation of a heterogeneous Mn(III)-hydroperoxo complex. *Chem. Eng. J.*, 2024, 500: 157135.

[215] Wang, J. L.; Hou, K. P.; Wen, Y. Z.; Liu, H. L.; Wang, H. L.; Chakarawet, K.; Gong, M.; Yang, X. J. Interlayer structure manipulation of iron oxychloride by potassium cation intercalation to steer H_2O_2 activation pathway. *J. Am. Chem. Soc.*, 2022, 144(10): 4294–4299.

[216] Hu, P. D.; Su, H. R.; Chen, Z. Y.; Yu, C. Y.; Li, Q. L.; Zhou, B. X.; Alvarez, P. J. J.; Long, M. C. Selective degradation of organic pollutants using an efficient metal-free catalyst derived from carbonized polypyrrole *via* peroxymonosulfate activation. *Environ. Sci. Technol.*, 2017, 51(19): 11288–11296.

[217] Li, X. Y.; Liu, J. H.; Lv, R. L.; Chu, Y. Y.; Lv, L.; Lu, J. H.; Zhang, W. M. Novel carbon-coated zirconium oxide nanocomposites enable ultrahigh oxidant utilization efficiency for selective degradation of organic contaminants. *Chem. Eng. J.*, 2023, 463: 142369.

[218] Zhao, Y.; Yu, L.; Song, C. Y.; Chen, Z. L.; Meng, F. Y.; Song, M. Selective degradation of electron-rich organic pollutants induced by CuO@Biochar: The key role of outer-sphere interaction and singlet oxygen. *Environ. Sci. Technol.*, 2022, 56(15): 10710–10720.

[219] Zhang, L.; Cheng, K.; Yang, Z. Z.; Zhang, Y.; Kubuki, S.; Bingham, P. A.; Yong, Y. C.; Zhang, B. F.; Duan, X. G. Deciphering the origin of higher shell coordination on single iron catalysts for resilient modulating persulfate oxidation into singlet oxygen pathway. *Adv. Funct. Mater.*, 2025, 35: 2417441.

[220] Zhang, L. L.; Chen, J. B.; Zhang, Y. L.; Xu, Y.; Zheng, T. L.; Zhou, X. F. Highly efficient activation of peracetic acid by nano-CuO for carbamazepine degradation in wastewater: The significant role of H_2O_2 and evidence of acetylperoxy radical contribution. *Water Res.*, 2022, 216: 118322.

[221] Guo, J. R.; Wang, Y. J.; Shang, Y. N.; Yin, K. X.; Li, Q.; Gao, B. Y.; Li, Y. W.; Duan, X. G.; Xu, X. Fenton-like activity and pathway modulation *via* single-atom sites and pollutants comediates the electron transfer process. *Proc. Natl. Acad. Sci. USA*, 2024, 121: e2313387121.

[222] Li, M.; Feng, Z. Y.; Yuan, X. Z.; Guo, C. X.; Qin, C. C.; Shu, Z. H.; Guo, Z. Y.; Ang, E. H.; Li, W. W.; Wu, Y. et al. Innovative asymmetric CoSA-N-$Ti_3C_2T_x$ catalysis: Unleashing superoxide radicals for rapid self-coupling removal of phenolic pollutant. *Angew. Chem. Int. Ed.*, 2025, 64: e202502307.

[223] Yan, H. C.; Lai, C.; Liu, S. Y.; Wang, D. B.; Zhou, X. R.; Zhang, M. M.; Li, L.; Ma, D. S.; Xu, F. H.; Huo, X. Q. et al. Insight into the selective oxidation behavior of organic pollutants *via* Ni-N_4-C mediated electron transfer pathway. *Chem. Eng. J.*, 2023, 473: 145253.

[224] Liang, L. H.; Cao, J. Z.; Zhang, Y. Y.; Liu, X. Y.; Li, J.; Yang, B.; Lv, W. Y.; Yang, Q.; Xing, M. Y. Selective adsorption of high ionization potential value organic pollutants in wastewater. *Proc. Natl. Acad. Sci. USA*, 2024, 121: e2403766121.

[225] Chen, Z.; An, F. L.; Zhang, Y. Y.; Liang, Z. Y.; Liu, W. Y.; Xing, M. Y. Single-atom Mo-Co catalyst with low biotoxicity for sustainable degradation of high-ionization-potential organic pollutants. *Proc. Natl. Acad. Sci. USA*, 2023, 120: e2305933120.

[226] Chen, L.; Yang, Z. C.; Qian, J. S.; Pan, B. C. Interaction between organic compounds and catalyst steers the oxidation pathway and mechanism in the iron oxide-based heterogeneous Fenton system. *Environ. Sci. Technol.*, 2022, 56(19): 14059–14068.

[227] Yin, K. X.; Shang, Y. N.; Chen, D. D.; Gao, B. Y.; Yue, Q. Y.; Xu, X. Redox potentials of pollutants determining the dominate oxidation pathways in manganese single-atom catalyst (Mn-SAC)/peroxymonosulfate system: Selective catalytic mechanisms for versatile pollutants. *Appl. Catal. B Environ.*, 2023, 338: 123029.

[228] Ren, W.; Xiong, L. L.; Yuan, X. H.; Yu, Z. W.; Zhang, H.; Duan, X. G.; Wang, S. B. Activation of peroxydisulfate on carbon nanotubes: Electron-transfer mechanism. *Environ. Sci. Technol.*, 2019, 53(24): 14595–14603.

[229] Yang, M. X.; Hou, Z. X.; Zhang, X.; Gao, B. Y.; Li, Y. W.; Shang, Y. N.; Yue, Q. Y.; Duan, X. G.; Xu, X. Unveiling the origins of selective oxidation in single-atom catalysis *via* co–N4–C intensified radical and nonradical pathways. *Environ. Sci. Technol.*, 2022, 56(16): 11635–11645.

[230] Hasan, Z.; Hwa, J. Removal of hazardous organics from water using metal-organic frameworks (MOFs): Plausible mechanisms for selective adsorptions. *J. Hazard. Mater.*, 2015, 283: 329–339.

[231] Wang, Y. M.; Zhang, P.; Lyu, L.; Li, T.; Hu, C. Preferential destruction of micropollutants in water through a self-purification process with dissolved organic carbon polar complexation. *Environ. Sci. Technol.*, 2022, 56(15): 10849–10856.

[232] Su, H. R.; Wei, Y.; Qu, X. L.; Yu, C. Y.; Li, Q. L.; Alvarez, P. J. J.; Long, M. C. Mechanistic inference on the reaction kinetics of phenols and anilines in carbon nanotubes-activated peroxydisulfate systems: Pp-LFERs and QSARs analyses. *Chem. Eng. J.*, 2020, 385: 123923.

[233] Liu, X. R.; Liu, Y.; Qin, H. H.; Ye, Z. W.; Wei, X. J.; Miao, W.; Yang, D. H.; Mao, S. Selective removal of phenolic compounds by peroxydisulfate activation: Inherent role of hydrophobicity and interface ROS. *Environ. Sci. Technol.*, 2022, 56(4): 2665–2676.

[234] Li, X. Y.; Pignatello, J. J.; Wang, Y. Q.; Xing, B. S. New insight into adsorption mechanism of ionizable compounds on carbon nanotubes. *Environ. Sci. Technol.*, 2013, 47: 8334–8341.

[235] Pignatello, J. J.; Mitch, W. A.; Xu, W. Q. Activity and reactivity of pyrogenic carbonaceous matter toward organic compounds. *Environ. Sci. Technol.*, 2017, 51(16): 8893–8908.

[236] Xie, Z. H.; He, C. S.; Zhou, H. Y.; Li, L. L.; Liu, Y.; Du, Y.; Liu, W.; Mu, Y.; Lai, B. Effects of molecular structure on organic contaminants' degradation efficiency and dominant ROS in the advanced oxidation process with multiple ROS. *Environ. Sci. Technol.*, 2022, 56: 8784–8795.

[237] Lian, L. S.; Yao, B.; Hou, S. D.; Fang, J. Y.; Yan, S. W.; Song, W. H. Kinetic study of hydroxyl and sulfate radical-mediated oxidation of pharmaceuticals in wastewater effluents. *Environ. Sci. Technol.*, 2017, 51(5): 2954–2962.

[238] Luo, S.; Wei, Z. S.; Dionysiou, D. D.; Spinney, R.; Hu, W. P.; Chai, L. Y.; Yang, Z. H.; Ye, T. T.; Xiao, R. Y. Mechanistic insight into reactivity of sulfate radical with aromatic contaminants through single-electron transfer pathway. *Chem. Eng. J.*, 2017, 327: 1056–1065.

[239] Lee, J.; von Gunten, U.; Kim, J. H. Persulfate-based advanced oxidation: Critical assessment of opportunities and roadblocks. *Environ. Sci. Technol.*, 2020, 54(6): 3064–3081.

[240] Zhou, Y.; Jiang, J.; Gao, Y.; Pang, S. Y.; Yang, Y.; Ma, J.; Gu, J.; Li, J.; Wang, Z.; Wang, L. H. et al. Activation of peroxymonosulfate by phenols: Important role of quinone intermediates and involvement of singlet oxygen. *Water Res.*, 2017, 125: 209–218.

[241] Kohantorabi, M.; Moussavi, G.; Giannakis, S. A review of the innovations in metal- and carbon-based catalysts explored for heterogeneous peroxymonosulfate (PMS) activation, with focus on radical *vs.* non-radical degradation pathways of organic contaminants. *Chem. Eng. J.*, 2021, 411: 127957.

[242] Wang, J. L.; Wang, S. Z. Reactive species in advanced oxidation processes: Formation, identification and reaction mechanism. *Chem. Eng. J.*, 2020, 401: 126158.

[243] Boualam, O.; Mardi, L.; El Alami, S.; Ibaghline, H.; Tanji, K.; El Gaidoumi, A.; Belaabed, R.; El Knidri, H.; Addaou, A.; Laajeb, A. Innovative use of iron-impregnated natural illite as a catalyst for phenol purification through Fenton, sono-Fenton, photo-Fenton, and sono-photo-Fenton technologies. *J. Environ. Chem. Eng.*, 2025, 13: 117333.

[244] Bellouk, H.; Danouche, M.; El Mrabet, I.; Tanji, K.; Khalil, F.; Nawdali, M.; El Ghachtouli, N.; Zaitan, H. Remediation of the landfill leachate of Fez city (Morocco) by sono-photo-Fenton process: Cost and phytotoxicity assessment. *J. Water Process. Eng.*, 2023, 56: 104565.

[245] Moradi, M.; Elahinia, A.; Vasseghian, Y.; Dragoi, E. N.; Omidi, F.; Mousavi Khaneghah, A. A review on pollutants removal by Sono-photo-Fenton processes. *J. Environ. Chem. Eng.*, 2020, 8: 104330.